Restoring cellular magnesium balance through Cyclin M4 protects against acetaminophen-induced liver damage

Restoring cellular magnesium balance through Cyclin M4 protects against acetaminophen-induced liver damage

Authors

Irene González-Recio[1], Jorge Simón[1,2], Naroa Goikoetxea-Usandizaga[1], Marina Serrano-Maciá[1], Maria Mercado-Gomez[1], Rubén Rodríguez-Agudo[1], Sofía Lachiondo-Ortega[1], Clàudia Gil-Pitarch[1], Carmen Fernández-Rodríguez[1], Donatello Castellana[3], Maria U Latasa[4], Leticia Abecia[5,6], Juan Anguita[2,5], Teresa C. Delgado[1], Paula Iruzubieta[7], Javier Crespo[7], Serge Hardy[8,9], Petar D. Petrov[10], Ramiro Jover[10], Matías A Avila[2,4], César Martín[11], Ute Schaeper[12], Michel L Tremblay[8,9], James W Dear[13], Steven Masson[14], Misti Vanette McCain[15], Helen Reeves[14,15], Raul J Andrade[2,16], M Isabel Lucena[2,17], Daniela Buccella[18*], Luis Alfonso Martínez-Cruz[1*], Mª Luz Martínez-Chantar[1,2*]

[1]Liver Disease Lab, Center for Cooperative Research in Biosciences (CIC bioGUNE), Basque Research and Technology Alliance (BRTA), Bizkaia Technology Park, Building 801A, 48160 Derio, Spain.

[2]Centro de Investigación Biomédica en Red de Enfermedades Hepáticas y Digestivas (CIBERehd), Carlos III National Health Institute, Madrid, Spain.

[3]Research & Development, Center for Cooperative Research in Biosciences (CIC bioGUNE), Basque Research and Technology Alliance (BRTA), Bizkaia Technology Park, Building 801A, 48160 Derio, Spain.

[4]Hepatology Programme, CIMA, Idisna, Universidad de Navarra, Avda, Pio XII, n 55, 31008 Pamplona, Spain.

[5]Inflammation and Macrophage Plasticity Laboratory, Center for Cooperative Research in Biosciences (CIC bioGUNE), Basque Research and Technology Alliance (BRTA), 48160 Derio, Bizkaia, Spain

[6]Departamento de Inmunología, Microbiología y Parasitología, Facultad de Medicina y Enfermería. Universidad del País Vasco/ Euskal Herriko Unibertsitatea (UPV/EHU). Barrio Sarriena s/n 48940. Leioa, Spain

[7]Gastroenterology and Hepatology Department, Marqués de Valdecilla University Hospital, Clinical and Translational Digestive Research Group, IDIVAL, Santander, Spain

[8] Department of Biochemistry, McGill University, Montréal, QC, Canada H3G 1Y6.

[9] Rosalind and Morris Goodman Cancer Research Centre, McGill Unversity, Montréal, QC, Canada H3A 1A3.

[10] Instituto de Investigación Sanitaria La Fé, Valencia, Spain

[11]Biofisika Institute (UPV/EHU, CSIC) and Department of Biochemistry and Molecular Biology, University of the Basque Country (UPV/EHU), 48940 Leioa, Spain

[12]Silence Therapeutics GmbH, Berlin, Robert Rössle Strasse 10, 13125, Berlin, Germany.

[13]Pharmacology, Toxicology and Therapeutics, Centre for Cardiovascular Science, University of Edinburgh, UK.

[14]The Liver Unit, Newcastle-upon-Tyne Hospitals NHS Foundation Trust, Newcastle upon Tyne NE7 7DN, UK.

[15]Northern Institute of Cancer Research, The Medical School, Newcastle University, Newcastle upon Tyne NE2 7DN, UK.

[16]Unidad de Gestión Clínica de Enfermedades Digestivas, Instituto de Investigación Biomédica de Málaga-IBIMA, Hospital Universitario Virgen de la Victoria, Universidad de Málaga, Málaga, Spain.

[17]Servicio de Farmacología Clínica, Instituto de Investigación Biomédica de Málaga-IBIMA, Hospital Universitario Virgen de la Victoria, UICEC SCReN, Universidad de Málaga, Málaga, Spain,

[18]Department of Chemistry, New York University, New York, New York 10003, United States.

[*]**Corresponding authors** María Luz Martínez-Chantar: email: mlmartinez@cicbiogune.es and Luis Alfonso Martínez-Cruz: email: amartinez@cicbiogune.es. Liver Disease lab CIC bioGUNE, Ed. 801A Parque Tecnológico de Bizkaia, 48160 Derio, Bizkaia, Spain and Daniela Buccella: email: dbuccella@nyu.edu Department of Chemistry, New York University, New York 10003, United States

Abstract

Acetaminophen (APAP) is one of the most widely consumed and prescribed drugs. APAP overdose is one of the leading causes of intrinsic drug-induced liver injury (DILI), acute liver failure (ALF), and liver transplantation in the Western world.

Mg^{2+}, essential for health, plays a role in virtually every process within the human cell. The cellular transporter family cyclin M, also known as CNNM, plays a key role in Mg^{2+} transport across the cell membranes in different organs. Here, we identified that the expression of CNNM4 is elevated in the liver of patients with APAP-induced liver injury (AILI), with a concomitant disturbance in serum Mg^{2+} levels. We demonstrated that, in the liver, APAP interferes with the Mg^{2+} mitochondrial reservoir via CNNM4, which affects ATP production and ROS generation, further boosting endoplasmic reticulum (ER) stress of the hepatocytes. Importantly, the CNNM4 mutant T495I showed no effect. Finally, a shift in localization of CNNM4 from membrane to ER was shown under APAP toxicity.

Therapeutic targeting of *Cnnm4* in the liver with nanoparticles and GalNAc-formulated siRNA provides efficient protection from AILI by restoring hepatocyte Mg^{2+} homeostasis and by inducing hepatocyte restoration. Our results suggest that inhibition of *Cnnm4* may represent an alternative route for the treatment of DILI..

Introduction

Magnesium, or Mg^{2+} in its ionized form, is one of the most abundant divalent cations in the cell and acts as a cofactor in hundreds of enzymatic reactions within the cell[1]. In mammals, the total cellular Mg^{2+} concentration is maintained in the mid-millimolar range[2]. The essential role that Mg^{2+} plays in mediating biochemical reactions at a cellular level explains why alterations in Mg^{2+} homeostasis in the body lead to various disorders, such as the development of inflammatory responses in diabetes and asthma, preeclampsia, atherosclerosis or heart damage[3]. Particularly in the liver, Mg^{2+} deficiency has been associated with the risk of developing NASH[4], cirrhosis, alcoholic-derived liver damage and hepatocellular carcinoma[5]. Restoring the correct balance of hepatic Mg^{2+} thus emerges as an attractive strategy for treating liver pathology. However, no effective approaches for adjusting intracellular Mg^{2+} concentrations are currently available[6].

At present, the contribution of dysregulated Mg^{2+} homeostasis to the development of drug-induced liver injury (DILI) remains unknown. Due to the unpredictable nature and poorly understood pathogenesis of DILI, it has become a significant health problem, estimated to affect 19 out of 100,000 citizens worldwide[7]. In this context, the abuse of acetaminophen (N-acetyl-p-aminophenol, paracetamol, APAP), the most commonly used drug in the USA, is responsible for almost 500 deaths annually from DILI, 100,000 calls to the US Poison Center, 50,000 emergency room visits, and 10,000 hospitalizations[8]. APAP overdoses account for 46% of all acute liver failures (ALF) in the USA and 40-70% of the cases in Europe[9].

To date, the only approved pharmacological treatment for APAP overdose and early stages of idiosyncratic DILI is N-acetylcysteine (NAC)[10,11]. However, NAC treatment is only effective within 20 hours of the overdose[12] and standard doses of NAC in patients with advanced liver injury may not be sufficient[13]. Therefore, new therapeutic approaches are needed in this field[14].

N-acetyl-p-benzoquinone imine (NAPQI) represents the most harmful molecule derived from APAP metabolism. Its overproduction depletes hepatic reduced glutathione and enhances oxidative stress, which can lead to liver necrosis[12]. In this context, perturbation of the cross-talk between mitochondria and endoplasmic reticulum (ER) plays a major role in the development of hepatocellular death. Both organelles share cellular events such as c-Jun N-terminal kinase (JNK) pathway activation, essential in ER, and mitochondrial oxidative stress. Alterations in JNK activity modify the permeability of mitochondrial membrane associated with alterations in calcium (Ca^{2+}) metabolism, perturbations in mitochondrial membrane potential, and loss of the ability to synthesize ATP[15]. Mitochondria-associated ER membranes (MAMs) are common specific domains that play a critical role in the local transfer of Ca^{2+} to maintain cellular functions[16]. APAP

intoxication leads to calcium depletion and the accumulation of misfolded proteins that activate an adaptive cellular response in this organelle[17]. In this context, protein homeostasis is maintained through the activation of two cellular processes, the so-called unfolded protein response (UPR) and autophagy- and proteasome-dependent proteolysis[18]. UPR activation involves three distinct pathways: inositol requiring 1α (IRE1α), PKR-like ER kinase (PERK), and activating transcription factor-6α (ATF6α)[19]. Importantly, the initial steps are characterized by increased gene expression of ER chaperones such as calreticulin, which binds Ca^{2+} in the ER, and the Ca^{2+} ATPase 2 (SERCA2), which pumps Ca^{2+} from cytosol into the ER[20]. Some authors suggest that ER stress is a late event after APAP overdose[21,22], whereas mitochondrial alterations, ATP depletion, JNK activation, oxidative stress, and miss-regulation of Ca^{2+} homeostasis are earlier events[21,23,24].

Previous studies[25] showed that mitochondria represent major intracellular reservoirs of Mg^{2+}. Mitochondrial Mg^{2+} release in whole cells occurs upon mitochondrial depolarization[25]. Perturbation of this mitochondrial Mg^{2+} levels then interferes with cellular energy metabolism and ATP production, sensitizing the cell to stress response[12]. Considering the protective properties of Mg^{2+} and the key role of mitochondria and ER in acute liver failure caused by APAP overdose, we evaluated the homeostasis of this cation under these conditions. The flux of Mg^{2+} across cell membranes is controlled by the activity and interplay of several Mg^{2+} transporters, such as mitochondrial RNA splicing 2 (MRS2)[26], cyclin M 1-4 (CNNM1-4)[27], transient receptor potential melastatin 6-7 (TRPM6-7)[28], membrane magnesium transporter (MMgT)[29] and magnesium transporter subtype 1 (MagT1)[29].

Our results show that in primary hepatocytes and in preclinical rodent models challenged with APAP, only the cyclin M4 (CNNM4) appears to be upregulated among all of these Mg^{2+} transporters. Importantly, patients who underwent APAP DILI also displayed high levels of hepatic CNNM4 expression and perturbation of Mg^{2+} serum levels. Although it is well established that CNNM4 plays a role in Mg^{2+} transport across cell membranes, its specific role in the liver and possible contribution to hepatic pathology remain largely unknown[30]. In the present work, we have investigated the contribution of CNNM4 to the pathology of AILI in *in vitro* and *in vivo* models. Suppression of *Cnnm4* expression in the liver restores hepatic Mg^{2+} content in mitochondria and ensures proper calcium influx into the ER, resulting in downregulated activation of the JNK pathway shared by both organelles. Conversely, overexpression of Cnnm4 increases susceptibility to liver injury, whereas the T495I mutant of CNNM4[31], unable to efflux Mg^{2+}, lacks this capability. APAP toxicity boosts the CNNM4 in the ER cellular localization. Thus, regulation of Mg^{2+} homeostasis by attenuating *Cnnm4* expression protects mitochondria and ER stress,

avoids necrosis, and consequently preserves liver function and protects against ALF. These results point to a new mechanism that has been underestimated in liver pathology, focusing on Mg^{2+} transport and the consequences of its modulation during DILI.

Methods

Human samples.

Serum biological samples from 4 control individuals with no liver diseases and tolerant to commonly used drugs attending routine work monitoring were used to measure magnesium levels (Hospital Virgen de la Victoria, Málaga, Spain). Twenty-four serum samples from patients with acute liver disease after a single acute APAP overdose with known time of drug ingestion were used to determine magnesium levels. A detailed characterization of the patients is summarized in Supplementary Table I (The Queen's Medical Research Institute). A total of 13 samples from explants of patients undergoing urgent liver transplantation for ALF resulting from acetaminophen overdose were evaluated for CNNM4 expression. The diagnosis was established by the Newcastle Hospitals NHS Foundation Trust (Newcastle, England) based on clinical data. Detailed descriptions of the patients are given in Supplementary Table II. The timing between overdose and the explant for the patients with hyper-acute liver failure (from paracetamol) was usually 3 days.

Finally 3 samples from healthy, non-obese organ transplant donors without liver lesions (Marqués de Valdecilla University Hospital, Santander, Spain), were used as controls for immunostaining analyses. The study was approved by the Research Ethics Committee of IDIVAL Cantabria 2017.052. Newcastle patient tissues were shared from the Newcastle biomedicine biobank (12/HE/0395), approved by the Newcastle Research Ethics Committee of North East Newcastle and North Tyneside. This study, EudraCT number 2017-000246-21 and ClinicalTrials.gov identifier NCT03177395, was approved by the UK medicines regulator, MHRA (25th April 2017) and West of Scotland Research Ethics Committee 1, Glasgow, UK (11th April 2017).

Animal model for acetaminophen-induced liver damage: Mice were starved for 12 hours and then given acetaminophen (APAP, Sigma Aldrich) by intraperitoneal injection in a single dose of 360 mg/kg. Animals were sacrificed at 24 and 48 hours after APAP overdose.

GalNAc siRNAs: GalNAc#1 and #2 comprise double stranded 19mer RNAs with 2'-O-methyl, 2'-fluoro-2'deoxy modifications and phrophorothioate bonds targeting *Cnnm4* linked to triantennary GalNAc unit. Non-targeting control siRNA conjugate represents a siRNA for Luciferase (Photinus pyralis) linked to the same GalNAc unit. *Cnnm4* molecules were designed, synthesized and purified by Silence Therapeutics GmbH, Berlin[32]

Results

Disturbance of Mg^{2+} homeostasis and hepatic overexpression of CNNM4 are observed in patients with DILI and in pre-clinical models of APAP-induced DILI.

Mg^{2+} homeostasis has been linked to liver function[5,33]. To investigate whether Mg^{2+} homeostasis could be dysregulated in patients with acetaminophen DILI, we evaluated Mg^{2+} serum levels in a cohort of these patients, characterized in Supplementary Table I. Mg^{2+} levels were significantly increased in patients with DILI (n = 24) versus controls (n = 4) (Figure 1A), suggesting that the flux of this cation may be aberrant in this pathological condition.

Preclinical animal models of APAP overdose have been developed that recapitulate many important aspects of human pathology. Evaluation of Mg^{2+} also shows increased serum levels in animals treated with a single dose of APAP 360 mg/kg for 48 hours compared with healthy animals (Figure 1B). These results support the original hypothesis that there is a link between DILI and disturbances in Mg^{2+} homeostasis. Despite significant progress in our knowledge of Mg^{2+} transport and homeostasis, more research is required to characterize the specific transporters implicated in Mg^{2+} flux in different physiological conditions. Several proteins have been identified as regulators of Mg^{2+} homeostasis in vertebrates, including magnesium transporter 1 (MagT1), mitochondrial RNA splicing 2 (MRS2), and transient potential receptor melastatin 6-7 (TRPM6-7), as well as the ancient cation divalent protein/cyclin M 1-4 (CNNM1-4) family. A full characterization of the liver profile of these transports was performed in mouse primary hepatocytes and human hepatocyte THLE-2 cells exposed to APAP for different time periods, as well as in a mouse model of APAP-induced liver injury. We found that *Cnnm4* at the mRNA level was remarkably increased in APAP overdose in both *in vitro* and *in vivo* models (Figure 1C-E). CNNM4 protein and mRNA expression levels were also significantly elevated in the livers of mice after APAP-induced liver injury (Figure 1F-H and Supplementary Figure 2A). To demonstrate the specificity of CNNM4 staining in liver sections, competitive analyses were performed with the pure protein. The results shown in Supplementary Figure 2B confirm the findings.

Given that the CNMMs were previously reported to be involved in maintaining Mg^{2+} homeostasis[34,27], we investigated whether CNNM4 could also be associated with susceptibility to hepatic toxicity in humans. We measured its expression in liver biopsies from control individuals and patients diagnosed with DILI as characterized in Supplementary Table II. Quantitative histological analysis demonstrated increased hepatic CNNM4 in patients with DILI relative to healthy controls (Figure 1I).

Overall, we provide strong evidence that hepatic CNNM4 expression is increased in DILI, which is also correlated with serum Mg^{2+} levels.

Targeting Cnnm4 resolves APAP toxicity in mouse and human hepatocytes.

Cell death is a main characteristic of DILI. APAP overdose triggers cell inflammation and cell death in the liver[35]. We observed that *Cnnm4* silencing reduced the extent of APAP-induced cell death, as assessed by TUNEL assay, while the remaining Cnnms failed to provide protection against the hepatocyte injury (Figure 2A, Supplementary Figure 3A-B). Importantly, the silencing of *Cnnm4* does not affect the other *Cnnms* (Supplementary Figure. 3C). Moreover, the protective role of CNNM4 silencing was also supported by trypan blue viability assay at 3 and 6 hours of APAP overdose (Supplementary Figure 3D). To support these initial findings a de novo in silico design and screen for highly active and specific *Cnnm4* siRNA molecules was performed. The best candidates were further characterized *in vitro* and *in vivo.*

Silencing of *Cnnm4* with two different siRNAs in human hepatocyte THLE-2 cells also reduced cell death assessed 3 hours after APAP treatment, evaluated by TUNEL and annexin V apoptosis and necrosis assays (Figure 2B), and 6 hours after treatment by TUNEL (Supplementary Figure 4A).

In addition, we employed GalNAc siRNA technology developed for gene silencing, in hepatocytes. *Cnnm4* siRNAs conjugated to triantennary N-acetylgalactosamine (GalNAc) are readily targeted to hepatocytes *in vitro* or *in vivo* by binding to the asialoglycoprotein receptor (ASGPR), which promotes specific and functional siRNA delivery by receptor mediated uptake[36].

Of relevance, the two GalNAc-conjugated *Cnnm4* siRNAs employed completely attenuated the induction of *Cnnm4* expression at two different concentrations by APAP, which led to a significant reduction of cell death at 3 hours, as evaluated by TUNEL and annexin V apoptosis and necrosis assays (Figure 2C) and at 6 hours after APAP overdose evaluated by trypan blue (Supplementary Figure 4B) and TUNEL (Supplementary Figure 4C). Importantly, the complementary approach, inducing CNNM4 expression by transfection of Cnnm4 cDNA (pDEST-26 expression plasmid), boosted the sensitivity of primary hepatocytes to APAP overdose, leading to higher values of TUNEL and annexin V apoptosis and necrosis assays (Figure 2D and Supplementary Figure 4D).

Considering the previous role described by CNNM4 as an extruder of Mg^{2+} in non-hepatic cells and the beneficial effect of this cation in liver disease[37,38], primary hepatocytes with and without Cnnm4 overexpression were supplemented with Mg^{2+} to mimic the potential therapeutic effect of this cation (Figure 2D). Mg^{2+} supplementation at different

concentrations was not able to counteract the damage caused by APAP (Supplementary Figure 4E) or Cnnm4 overexpression, measured by TUNEL and annexin V apoptosis and necrosis assays (Figure 2D).

Previous data showed that amino acid substitution of CNNM4-T495I in the CBS domains of CNNM4 completely abrogates Mg^{2+} efflux[31]. In order to understand its effect in primary hepatocytes under APAP treatment, the Cnnm4-T495I mutant was overexpressed. Importantly, Cnnm4-T495I overexpression did not induce any apoptotic response, based on the lack of inhibition in efflux activity (Figure 2E and Supplementary Figure 4F-G).

Finally, to evaluate APAP metabolism and bioactivation after *Cnnm4* knockdown, the activity of CYP2E1 was evaluated in primary hepatocytes after 3 hours of treatment. APAP significantly reduced CYP2E1 activity, as described previously[39], and high levels of Cnnm4 showed the same tendency (Supplementary Figure 4H). However, CYP2E1 activity was recovered in the absence of *Cnnm4,* while no type of modulation was observed with Cnnm4-T495I (Supplementary Figure 4H).

Together, these data indicate that silencing of *Cnnm4* confers resistance to APAP-mediated necrosis, whereas overexpression of Cnnm4 confers sensitization to liver injury. Mg^{2+} supplementation failed to counteract APAP-mediated toxicity in the presence of Cnnm4. The death mutant Cnnm4-T495I showed no effect on cell death.

Targeting Cnnm4 restores Mg^{2+} flux and reduces mitochondrial dysfunction in primary hepatocytes.

Mitochondrial dysfunction triggered by APAP is one of the mechanisms that causes cell death in the liver[40]. First, we observed that the mitochondrial potential membrane in primary hepatocytes was restored in the absence of *Cnnm4* (Figure 3A). Mitochondrial OXPHOS[41] monitored by seahorse analysis of hepatocytes under APAP exposure and *Cnnm4* silencing showed a higher oxygen consumption rate (OCR) in these conditions and reestablished the reservoir of ATP linked to respiration, avoiding the liver necrosis mediated by APAP overuse (Figure 3B-C). Moreover the absence of *Cnnm4* also resulted in a marked reduction in ROS production, assessed by MitoSOX, in APAP-treated primary hepatocytes (Figure 3D). However, Cnnm4 overexpression induced mitochondrial ROS (Figure 3E), while Cnnm4-T495I reduced ROS cellular content in comparison with APAP (Figure 3E).

The function of CNNM4 in the liver under metabolic disturbances has been addressed[30]. Some authors have described CNNM4 in the intestinal epithelium as an extruder that exchanges intracellular Mg^{2+} with extracellular Na^{+}, while others have pointed to its role as a Mg^{2+} mediator of other transcellular transporters[37,42]. In order to further assess the relevance of the Mg^{2+} flux in hepatocytes under *Cnnm4* silencing conditions, relative

intracellular Mg^{2+} levels were analyzed by mitochondrial-specific (Mg-S-TTP-AM)[30] and cytosolic-specific (Mg-S-AM)[30,43] labelling in primary hepatocytes after APAP administration (Figure 3F). As expected, Mg^{2+} content was decreased under hepatotoxic exposure, mainly in the mitochondria (Figure 3F). On the other hand, *Cnnm4* silencing promoted restoration of normal Mg^{2+} levels in these organelles and in the cytoplasm, indicating that in the liver CNNM4 functions as a Mg^{2+} extruder (Figure 3F). Mg^{2+} content was also measured in the presence of 5 and 20 mM of this cation under APAP treatment. Mg^{2+} mitochondrial content was not reestablished under these conditions (Figure 3G). Finally, Cnnm4 overexpressed in primary hepatocytes significantly reduced the levels of mitochondrial-specific Mg^{2+} (Mg-S-TTP-AM)[30] and cytosolic-specific Mg^{2+} (Mg-S-AM) (Figure 3H). In the case of Cnnm4-T495I mutant, increased cytosolic and mitochondrial Mg^{2+} levels were observed in the hepatocytes(Figure 3H).

Thus silencing of *Cnnm4* reduces mitochondrial ROS and restores Mg^{2+} mitochondrial levels under APAP toxicity.

Cnnm4 reduces endoplasmic reticulum stress in primary hepatocytes.

Cell death is an extremely coordinated phenomenon involving multiple signaling pathways with interplays and crosstalk between ER and mitochondria[44]. To evaluate ER activity[19] in primary hepatocytes under APAP treatment, we examined Ca^{2+} release capacity in the ER by using the Grynkiewicz[45] method and a specific FURA-2 labelling. A lack of *Cnnm4* led to a more functional hepatic ER with a higher release of Ca^{2+} under the different stimuli, including thapsigargin (a specific inhibitor of the ER SERCA pump)[46,47] and ATP (which triggers Ca^{2+} release through P2Y receptor)[48] (Figure 4A) (Supplementary Figure 5A).

Regarding the kinases involved in the stress response mediated by APAP treatment, JNK activation has emerged as a crucial event in acute liver injury. A decreasing tendency of activated JNK levels was observed 1 hour after APAP administration in si*Cnnm4*-treated hepatocytes compared to controls (Figure 4B).

Therefore, to investigate whether *Cnnm4* siRNA treatment could reduce ER stress by APAP-induced damage, primary hepatocytes were treated with APAP for a 6 hours-time course. The development of ER stress was observed in control cells under APAP treatment, while hepatocytes treated with si*Cnnm4* were significantly protected, as assessed by the mRNA of *Atf6*, *Chop*, *Xbp1,* and *Grp78* (Figure 4C). In contrast, the overexpression of Cnnm4 affected the levels of genes related to ER stress in the hepatocytes, whereas Cnnm4 T495I did not have the same effect as the WT Cnnm4 (Figure 4C).

To further identify perturbations in ER function modulated by CNNM4 in the presence of APAP, primary hepatocytes were also labeled with an ER-tracker that binds to the ATP-sensitive K^+ channels. Previously data have shown that the ER K^+ channel activity is induced under stress[49]. Fluorescence images confirmed the beneficial effect of *Cnnm4* knockdown and revealed decreased numbers of red-stained cells under APAP exposure (Figure 4D). However, Cnnm4 overexpression significantly modulated ER activity, while Cnnm4 T495I did not exert the same effect as the WT Cnnm4 (Figure 4F).

Finally, hepatocytes treated with a well-known inducer of ER stress, tunicamycin[18], showed a decrease in tunel assay when *Cnnm4* was knocked down. These results highlight the important role of CNNM4 in hepatocytes under ER stress (Supplementary Figure 5B).

Thus, we found that *Cnnm4* deficiency alleviates the APAP-mediated ER stress through its Mg^{2+}effluxer activity in primary hepatocytes.

Cnnm4 silencing overcomes APAP toxicity in preclinical animal models.

Silencing the expression of specific genes by RNA interference has been employed as a therapeutic tool for liver diseases in a number of clinical trials[50]. To determine the protective effect of silencing *Cnnm4* expression, WT mice were treated with a toxic dose of APAP, and 24 hours later siRNA *Cnnm4* or an unrelated control (siCtrl) was formulated with Invivofectamine 3.0 and administered by tail vein injection (i.v.). Mice were sacrificed 24 hours later and tested for gene expression levels of *Cnnm1-4*. The gene profile performed in the liver of these animals showed that, first of all, *Cnnm4* was the only transporter elevated after APAP-induced injury, and only *Cnnm4* was specifically silenced, although not completely, upon treatment (Figure 5A and Supplementary Figure 6A-C). Silencing of *Cnnm4* at the basal level showed no effects, as indicated by hematoxylin and eosin (H&E), alanine transaminase (ALT) and aspartate transaminase (AST) levels, and inflammatory responses (Supplementary Figure 6D-F), with the exception of serum Mg^{2+} levels (Supplementary Figure 6G). However, following APAP overdose, H&E staining and TUNEL assay revealed the presence of necrotic areas in the siCtrl-treated cohort caused by the APAP overdose, whereas in the si*Cnnm4*-treated cohort, the liver parenchyma was significantly less disturbed by necrotic areas (Figure 5B-C). Importantly, the analysis of serum transaminases revealed that si*Cnnm4* treatment significantly reduced their levels (Figure 5D). To further assess liver injury, we performed DHE staining to detect intracellular superoxide formation in liver sections. Knocking down *Cnnm4* in the liver of APAP-treated mice significantly reduced oxidative stress (Figure 5E). Accordingly, glutathione species in liver tissues were analyzed. While

the GSSG/GSH ratio tended to increase under APAP overdose, the absence of *Cnnm4* reduced this oxidative ratio (Supplementary Figure 6H).

The inflammatory response is a well-known process during DILI[40]. The analysis of F4/80 staining showed lower numbers of macrophages in Cnnm4-targeted livers (Figure 5F). This decreased inflammation in the si*Cnnm4* treatment group was further supported by the attenuation of mRNA expression levels of inflammatory cytokines *Tnf*, chemokine (*Cxcl-1*), and chemokine receptor (*Ccl2*) (Supplementary Figure 6I). The analysis of serum TNF and IL6 determined by ELISA confirmed the rescue of the inflammatory process under *Cnnm4* silencing conditions (Supplementary Figure 6J). Finally, these data are in agreement with the significantly increased of Mg^{2+} serum level in APAP-treated mice, while the silencing of *Cnnm4* reduced the Mg^{2+} levels (Figure 5G). These data confirm the modulation of Mg^{2+} flux by *Cnnm4* silencing *in vivo.*

To further investigate the beneficial effects of silencing *Cnnm4* specifically in the liver, a GalNAc formulation was used in mice treated with a single dose of APAP 360mg/kg for 24 hours. Animals were sacrificed 48 hours after APAP treatment, and CNNM4 levels were assessed by RNA and protein expression, showing significant reductions (Figure 5H and Supplementary Figure 7A-B). Necrotic areas, TUNEL assay, and transaminase levels were evaluated (Figure 5I-K). In addition, the inflammatory response was examined (Figure 5L). The results show a statistical reduction in liver injury with GalNAc *Cnnm4* siRNA treatment. These data are consistent with the modulation of Mg^{2+} levels in the presence of GalNAc *Cnnm4* siRNA (Figure 5M). These results bring the treatment of DILI closer to that of GalNAc *Cnnm4* acting specifically in the liver.

N-acetylcysteine (NAC) is the only available therapy for the treatment of patients with APAP overdose, but if administered after 8 hours of APAP uptake, its efficacy decreases dramatically[10,11,12,13]. To compare the beneficial effects of NAC versus *Cnnm4* silencing, control mice were administered APAP and treated with NAC 24 hours later. Then, 48 hours after APAP administration, hepatoxicity was examined. In contrast to si*Cnnm4* treatment, liver injury, as determined by histology (Supplementary Figure 7C), and serum AST and ALT (Supplementary Figure 7D), were not affected by NAC treatment.

Together, these results show that in this mouse model, applying *Cnnm4* siRNA 24 hours after administering an overdose of APAP, a time point when it is non-treatable by NAC, can ameliorate necrosis and inflammatory response in the liver.

It is well established that CNNM4 is a Mg^{2+} transporter highly expressed in the colon epithelia[37]. To determine the liver specificity of *Cnnm4* targeting, CNNM4 levels were measured in the intestine. The expression of CNNM4 increased by APAP treatment in both the control and *Cnnm4* siRNA experimental groups, without significant differences (Supplementary Figure 8A). Moreover, silencing of *Cnnm4* in healthy mice did not modulate its expression in the intestine, thus excluding non-hepatic sites of action for such silencing (Supplementary Figure 8B). To further investigate whether liver-specific *Cnnm4* silencing could also be associated with cell differentiation in the colon epithelia, making them more vulnerable to injury, we analyzed intestinal permeability by FITC-dextran. We identified a deficiency in the intestinal integrity of mice treated with APAP, whereas si*Cnnm4* tended to reduce permeability levels closer to normal (Supplementary Figure 8C). Finally, to determine the specificity of CNNM4 IHC staining in the intestine, competitive assays were conducted with the pure protein validating our findings (Suppl Fig. 8D).

Together these results show that inhibiting *Cnnm4* expression in the liver after APAP administration does not produce any negative effects on the intestinal barrier function.

Targeting Cnnm4 in preclinical APAP model ameliorates ER stress and mitochondrial ROS through Mg^{2+} modulation.

To further interrogate the mechanism underlying *Cnnm4* silencing in DILI, high-throughput proteomics analysis was performed in liver extracts from mice administered an acetaminophen overdose in the presence or absence of this gene and in a control group. Volcano plots show the more representative proteins modulated in the absence of CNNM4 (Figure 6A). For more specific detail, the top-50 up- and downregulated proteins linked to CNNM4 presence under APAP treatement were represented in a heatmap (Supplementary Figure 9A). The Database for Annotation, Visualization, and Integrated Discovery (DAVID) was used to analyze the major signaling pathways altered by *Cnnm4* knockdown (Figure 6B). Processes downregulated by the absence of *Cnnm4* included those involved in mitochondrial membrane and ATP metabolic pathways, and in particularly gene ontology families related to ER activity, protein transport, misfolding, and their catabolic regulation (Figure 6B). In contrast, pathways involved in the regulation of cytokine-mediated signaling; interferon alpha, implicated in liver regeneration, among others processes; and the response to interleukin 10 appeared to be overrepresented in these circumstances (Figure 6B).

Based on these data, first we investigated whether reduction of *Cnnm4* expression *in vivo* protects against liver injury by modulating the three major pathways mediated by

the ER-resident transmembrane proteins ATF6, IRE1 and PERK. We found that a lack of *Cnnm4* attenuated the translation of the splicing of *Xbp1* mRNA, related to IRE1 activation (Figure 6C). These results are in accordance with the observed reduction of *Chop* (Figure 6C). Moreover, we observed a decreasing tendency of *Atf6* and *Grp78* levels silencing *Cnnm4* (Figure 6C*)*. Accordingly, APAP stimulated the phosphorylation of EIF2alpha, which was attenuated by si*Cnnm4* (Figure 6D).

Moreover, the GalNAc *Cnnm4* siRNA therapeutic approach under APAP treatment *in vivo* also led to a reduction in ER stress, as shown in Figure 6E-F.

These results suggest that *Cnnm4* silencing treatment restores normal Mg^{2+} homeostasis and reduces the ER stress triggered by APAP overdose in *in vivo* animal models of APAP-induced liver failure.

To better understand the effects mediated by CNNM4 on ER activity under APAP exposure, the cellular localization of this protein was analyzed in the liver of DILI animal models (Figure 6G). Highly enriched fractions from liver tissue allowed us to monitor the downregulation of CNNM4 levels in the membrane fraction in the presence of APAP compared with increased ER under these conditions (Figure 6G). The mitochondrial fraction did not exhibit CNNM4.

Finally, considering the interplay between ER and mitochondria and the disturbance of Mg^{2+} content in the mitochondria under *Cnnm4* silencing, mitochondrial respiration was evaluated in mitochondria from APAP-treated mice with siRNA GalNAc *Cnnm4* and unrelated control (Figure 6H). ROS production and ATP levels were evaluated in hepatocytes derived from APAP-treated mice and those under GalNAc *Cnnm4* treatment (Figure 6I-J). The data identified that GalNAc *Cnnm4* also improved mitochondrial activity and its bioenergetics. In this context, a significantly reduction in ER tracker was also identified (Figure 6K).

CNNM4 knockdown induced liver regeneration in preclinical APAP model.

Increased ATP levels in the liver after injury could facilitate liver regeneration, an energetically demanding process[12]. To further assess the impact of ATP production under *Cnnm4* silencing in liver regeneration, the proliferative response was evaluated in mice subjected to liver damage 48 hours after APAP overdose. Analysis of cyclin D1 and A2 gene expression in liver tissue showed increased levels in si*Cnnm4*-treated mice (Figure 7A). In addition, *Cnnm4* silencing induced proliferating cell nuclear antigen (PCNA) staining in liver sections (Figure 7B). Further analysis of the upstream regulators mediating liver regeneration after APAP injury revealed that hepatocyte growth factor (HGF), considered critical for hepatocyte proliferation[51], was significantly increased

under these conditions (Figure 7C). Liver regeneration evaluated at an early time, 36 hours for mice administered APAP, and 12 hours later of GalNAc *Cnnm4* injection resulted (Figure 7D) in a reduction of p21 cell cycle arrest (Figure 7E) and significant activation of phospho c-Met (Fig 7F). Downregulation of the inflammatory response mediated by F4/80 was identified under GalNAc *Cnnm4* silencing (Supplementary Figure 10A-E)

Thus, targeting *Cnnm4* at late phases of APAP toxicity can induce a regenerative response in the liver, thus counteracting the damage produced after the administration of this drug.

Discussion

DILI is a clinical and pathological term for liver injury caused by various medications, leading to abnormalities in liver tests or liver dysfunction. DILI is one of the leading causes of acute liver failure, which can result in the need for liver transplantation or even in death[52]. APAP overdose is one of the principal causes of DILI[53], with necrosis as the primary pathway of hepatocyte cell death. Understanding the mechanisms behind APAP-mediated toxicity is therefore essential in order to overcome liver damage with appropriate therapies. In this work, we took the challenge of identifying Mg^{2+} perturbations in DILI patients and studied the impact by modulating Mg^{2+} in preclinical AILI models. Our findings reveal that CNNM4 is a major mediator of Mg^{2+}efflux from liver to extracellular compartments. We show that *Cnnm4* silencing under APAP exposure results in the restoration of Mg^{2+} levels within the mitochondria, ameliorating ER stress and protecting mitochondria functionality (Figure 8). Our observation that hepatic CNNM4 is upregulated in the preclinical animal models as well as in ALF patients who underwent liver transplant due to acetaminophen overdose supports this premise. These results pave the way toward considering CNNM4 as a new therapeutic target for the treatment of this common hepatotoxic condition.

Mg^{2+} is essential for health and plays a role in virtually every process within the human cell. Given such important functions, it is clear that perturbations in intracellular Mg^{2+} concentrations could have serious implications for the physiological functioning of cells. Dysfunction of Mg^{2+} handling is linked to different pathologies, including liver diseases[5], diabetes[3], hypertension[3], and cardiovascular diseases. Here, we show that CNNM4 levels are elevated in primary hepatocytes challenged with APAP in the liver of mice after APAP overdose, and in liver tissue from DILI patients with ALF. Thus, APAP appears to trigger Cnnm4 overexpression in the liver, with a concomitant Mg^{2+} efflux from the hepatocytes to the extracellular media. Consistent with this, serum Mg^{2+} levels both in the APAP overdose animal model and in APAP DILI patients were increased. Importantly, under conditions of liver toxicity, CNNM4 appears to accumulate in the ER[54]. Indeed, an analysis by the SubCons webserver identified a signal peptide responsible for the ER localization of CNNM4. High-throughput proteomics analysis revealed that in the absence of *Cnnm4*, pathways related to ER activity, protein transport, misfolding, and their catabolic regulation were mainly affected under APAP overdose. CNNM4 upregulation in the ER may explain the Mg^{2+} disturbances observed in the hepatocytes in ALF.

The pattern of Mg^{2+} levels in primary hepatocytes, determined by mitochondrial-specific (Mg-S-TTP-AM)[30] and cytosolic-specific (Mg-S-AM)[43] labelling, showed that CNNM4 acted as an effluxer reducing Mg^{2+} levels in the cell and in the mitochondria. There are several signaling mechanisms linking ER stress and mitochondrial cell death pathways. MAMs are the interaction zones between the two organelles that allow rapid exchange of molecules; among them, Ca^{2+} maintains cellular function and cellular health. Thus, the presence of CNNM4 in the ER under APAP toxicity probably dysregulates ER Ca^{2+} homeostasis and induces a misfolding protein response and mitochondrial ROS. The overexpression of Cnnm4 and the results obtained in the presence of the inactive mutant T495I[31] unable to induce Mg^{2+} efflux support the role of CNNM4 in the ER. Indeed, targeting *Cnnm4* in hepatocytes under APAP treatment preserves ER activity and reduces the stress mediated by this toxicant ameliorating cell death. This effect appears to be dependent on the cells in which the modulation of CNNM4 occurs. Previous work has shown that silencing of *Cnnm4* in intestinal epithelial cells triggers an oxidative stress response[55]. Hepatocytes, which are rich in mitochondria, have a high oxidative capacity[56]. This characteristic probably leads to a differential response under *Cnnm4* knockdown. Therefore, *Cnnm4* should specifically be silenced in certain cell types, as is the case with GalNAc si*Cnnm4* in the hepatocytes.

Mg^{2+} deficiency has been previously reported in patients with liver disease, although the relationship between this cation, liver function, and the disease has not been fully elucidated[53]. CNNM4, which is upregulated in NAFLD patients, has been described as a master regulator of VLDL export in this pathology, mediated by activation of the microsomal transfer protein found in the ER[30]. Under steatotic conditions[30] or in primary hepatocytes where Cnnm4 was overexpressed or treated with APAP, Mg^{2+} supplementation did not result in any recovery effect or protection from the necrotic processes. Then, hepatic *Cnnm4* silencing appeared to be required for amelioration of Mg^{2+} disturbances in liver disease due to its efflux activity. In this context, it is important to highlight that common to the two pathologies, NAFLD and ALF, is that that reticulum stress is one of the main altered pathways through which CNNM4 can exert its therapeutic effects.

Liver regeneration plays a critical role in resolving APAP-induced ALF[57].Cellular ATP levels are essential for liver regeneration[58]. Hepatic cell death triggered by APAP is closely related to cellular ATP deprivation caused mainly by mitochondrial dysfunction. In the absence of *Cnnm4*, ATP levels increase, favoring proliferation and preventing hepatic necrosis, which is mainly due to decreased mitochondrial ROS and reticulum stress. Additionally, *Cnnm4* deficiency in APAP injury leads to upregulation of HGF and

consequent phosphorylation of c-MET. HGF has been described to play a fundamental role in regeneration after ALF[57]. Moreover, the absence of *Cnnm4* under these experimental conditions also leads to decreased p21 levels. p21 has been directly linked with the impairment liver regeneration observed in patients after severe APAP-induced liver injury in patients[59]. This reduction in p21 along with increased cyclin D1 and PCNA levels suggests that the absence of *Cnnm4* enhances the regenerative response in ALF.

NAC is the only currently available effective therapy that can be deacetylated to cysteine and subsequently metabolized to GSH[54,60], although it has a limited therapeutic window. Thus, more effective therapeutic interventions are urgently needed. Our data have shown that at the time *Cnnm4* silencing appears to have therapeutic value in an ALF animal model, NAC is not a treatment option.

Overall, our results identified CNNM4 in the liver as a major effluxer responsible for Mg^{2+} dysregulation in ALF. The enrichment of CNNM4 in the ER justifies the stress response and mitochondrial dysfunction observed in *in vitro* and *in vivo* models of APAP-mediated hepatotoxicity. Our data demonstrate that *Cnnm4* inhibition represents a novel therapeutic option, even after 24 hour overdose of APAP, with additional benefits for liver regeneration and recovery from injury.

Acknowledgments

This work was supported by Ministerio de Ciencia, Innovación y Universidades MICINN: PID2020-117116RB-I00 and RTI2018-096759-1-100 integrado en el Plan Estatal de Investigación Cientifica y Técnica y Innovación, cofinanciado con Fondos FEDER (to MLM-C and TC-D respectively), Ministerio de Ciencia e Innovación CONSOLIDER-INGENIO 2010 Program Grant CSD2008-00005 (to LAM-C); Spanish Ministry of Economy and Competitiveness Grant BFU2013-47531-R, BFU2016-77408-R (MINECO/FEDER, UE); Asociación Española contra el Cáncer (MLM-C, TC-D), Fundación Científica de la Asociación Española Contra el Cáncer (AECC Scientific Foundation) Rare Tumor Calls 2017 (to MLM-C), La Caixa Foundation Program (to MLM-C), Fundacion BBVA UMBRELLA project (to MLM-C), Plataforma de Investigación Clínica-SCReN (PT17 0017 0020) (to MI-L), programa retos RTC2019-007125-1 (to M.L.M.-C, J.S), Proyectos Investigacion en Salud DTS20/00138 (to M.L.M.-C, J.S), ERA-Net E-Rare EJP RD Joint Translational Call for Rare Diseases FIGHT-CNNM2 (EJPRD19-040) and from Instituto Carlos III, Spain (REF G95229142) (to L.A.M-C), US National Institutes of Health under grant CA217817 (to DB), Ciberehd_ISCIII_MINECO is funded by the Instituto de Salud Carlos III. We thank MINECO for the Severo Ochoa Excellence Accreditation to CIC bioGUNE (SEV-2016-0644) and PhD fellowship from MINECO (REF BES-2017-080435) awarded to IG-R. The collection and storage of patients tissues was supported by the Newcastle Biomedicine Biobank and the European Community's Seventh Framework Programme (FP7/2001–2013). Finally, we would like to acknowledge Begoña Rodríguez Iruretagoyena for the technical support provided.

Author contributions

Conceptualization: IG-R, LAM-C, MLM-C, DB
Funding acquisition: TC-D, LAM-C, MLM-C
Experiments: IG-R, JS, NG-U, MS-M, MM-G, RR-A, SL-O, CG-P, CF-R, D-C, MU-L, LA, JA, TC-D, PI, JC, SH, PD-P, RJ, MA-A, CM, US, ML-T, JW-D, S-M, M-VM, H-R, RJ-A, MI-L
Supervision: LAM-C, MLM-C, DB
Writing – Original draft, review and editing: IG-R, LAM-C, MLM-C, DB

All authors have revised and approved the final version of the manuscript

Additional information

Ute Schaeper is employed by Silence Therapeutics GmbH.

Figure 1. Cyclin M4 (CNNM4) is overexpressed in DILI patients and pre-clinical animal models caused by APAP.

A. Magnesium serum levels determination in a cohort of AILI patients (n=24) compared to a group of healthy donors (n=4). Data are shown as mean ± SEM. ***P < 0.001 (Student's test) **B.** Magnesium serum levels was determined in a control group animals (n=4). and those treated with a single dose of APAP 360mg/kg for 48 hours (n=4). Data are shown as mean ± SEM. *P < 0.05 (Student's test) **C-E.** Changes in mRNA levels of *Cnnm1, Cnnm2, Cnnm3, Cnnm4, Trpm6, Trpm7, Mrs2, Mmgt1 and Magt1* in **(C)** WT hepatocytes under APAP 10 mM compared to a control group (Ctrl) for 1h, 3h and 6h **(D)** THLE2 cell line **(E)** and the experimental groups of APAP 360mg/kg (n=4) mice compared to a healthy group (n=4) at 48h. Data are shown as mean **F.** Liver immunohistochemical staining and respective quantification of CNNM4 was determined in the experimental groups of APAP 360mg/kg for 24h (n=4) and 48h (n=4) animal models compared to a healthy group (n=4). Scale bar correspond to 50 µm. **G.** mRNA levels *Cnnm4* and **H.** protein expression levels of CNNM4 in a animals treated with a single dose of APAP 360mg/Kg for 24h (n=4) and 48h (n=4) compared to a healthy group (n=4), β-ACTIN was used as a loading control. Data are shown as mean ± SEM. *P < 0.5, **P < 0.01 (Student's test) **I.** Liver immunohistochemical staining and respective quantification of CNNM4 was determined in a cohort of AILI (n=13) patients compared to a healthy group (n=3). Scale bar correspond to 100 µm. Values are represented as mean ± SEM. *P < 0.05, **P < 0.01, ***P < 0.001 (Student's test).

Figure 2. Silencing CNNM4 protects against APAP toxicity in *primary and human hepatocytes*

A. Cell death was evaluated using TUNEL in WT hepatocytes under APAP overdose for 3h and treated with a siRNA *Cnnm1*, *Cnnm2*, *Cnnm3* and *Cnnm4* or an unrelated control (siCtrl) compared to a control group (Ctrl). Scale bar correspond to 50 µm. **B.** Cell death, apoptosis and necrosis reponse were evaluated using TUNEL and Annexin V Apoptosis and necrosis assay respectively in THLE2 cell line under APAP overdose for 3h and treated with two different siRNA sequences of *Cnnm4* and compared to a control group (Ctrl). **C.** Cell death, apoptosis and necrosis reponse were evaluated using TUNEL and Annexin V Apoptosis and necrosis assay respectively were evaluated in primary murine hepatocytes treated with different GalNAc *Cnnm4* siRNAs (GalNAc#1 and GalNAc#2) at different concentrations 1nM and 10nM and exposed to APAP for 3 hours compared to untreated control group (Ctrl) **D.** Cell death, apoptosis and necrosis response were evaluated using TUNEL and Annexin V Apoptosis and necrosis assay in WT hepatocytes under APAP overdose for 3h with and without 5mM of Mg^{2+}, overexpressing Cnnm4 and overexpressing Cnnm4 with Mg^{2+} compared to a control group (Ctrl). **E.** Cell death, apoptosis and necrosis response were evaluated using TUNEL and Annexin V Apoptosis and necrosis assay in WT hepatocytes under APAP overdose for overexpressing Cnnm4 and overexpressing the mutant Cnnm4 T495I and compared to a control group (Ctrl). Values are represented as mean ± SEM. *P < 0.05, **P < 0.01, ***P < 0.001 (Student's test). Quadrupled were used for experimental condition.

Figure 3. CNNM4 silencing in hepatocytes reduces mitochondrial dysfunction under APAP toxicity

A. The mitochondrial membrane potential was determined in WT hepatocytes upon 3h of APAP overdose and treated with a siRNA *Cnnm4* or an unrelated control. **B.** Basal respiration using seahorse assay in primary hepatocytes and after 3h of APAP administration. **C.** Mitochondrial ATP production and linked respiration in primary hepatocytes under APAP overdose for 3h. The mitochondrial Reactive Oxygen Species was determined in WT hepatocytes upon 1h and 3h of APAP treatment using MitoSOX staining and treated with **D.** siRNA *Cnnm4* or an unrelated control and **E.** Cnnm4 and Cnnm4 T495I overexpression. Relative intracellular Mg^{2+} determination by mitochondrial-specific labelling and cytosolic-specific labelling in primary hepatocytes under APAP overdose for 3h and treated with **F.** a siRNA *Cnnm4* or an unrelated control (siCtrl) compared to a control group (Ctrl). **G.** 5mM and 20mM Mg^{2+} supplementation. **H.** Cnnm4 and Cnnm4 T495I overexpression compared to a control group (Ctrl). Quadrupled were used for experimental condition. Values are represented as mean ± SEM. *P <0.05, **P < 0.01, ***P < 0.001 (Student's test)

Figure 4. CNNM4 silencing in hepatocytes reduces endoplasmic reticulum stress under APAP toxicity

A. Calcium (Ca^{2+}) release capacity by ER with thapsigargin and ATP upon time under APAP overdose for 3h treated with a siRNA *Cnnm4* or an unrelated control (siCtrl) compared to a healthy group (Ctrl). **B.** Western blot analysis of phospho-JNK1/JNK2 (Thr183, Tyr185) (pJNK) and SAPK/JNK (Thr183, Tyr185) ratio, β-ACTIN was used as a loading control under APAP overdose for 1h. **C.** mRNA levels of *Atf-6, Chop, X-box binding protein 1 (Xbp1s/Xbp1u)* and binding immunoglobulin protein (*Grp78)* for 6h under APAP overdose and treated with (a) a siRNA *Cnnm4* or an unrelated control (siCtrl) compared to a control group (Ctrl). (b) Cnnm4 and Cnnm4 T495I overexpression compared to a control group (Ctrl). **D** ER tracker red staining with respective quantification in primary hepatocytes for 3h under APAP overdose and treated with a siRNA *Cnnm4* or an unrelated control (siCtrl) compared to a control group (Ctrl) and **E.** ER tracker red staining with respective quantification in primary hepatocytes for 3h under APAP overdose and treated with Cnnm4 and Cnnm4 T495I overexpression. Scale bar correspond to 100 µm. Quadrupled were used for experimental condition. Values are represented as mean ± SEM. **P* < 0.05, ***P*<0.01, ****P*<0.001 (Student's test)

Figure 5. CNNM4 silencing prevents hepatotoxicity mediated by APAP overdose in *in vivo* models.

A-F WT mice were treated with a single dose of APAP 360 mg/kg by intraperitoneal injection and 24h after siRNA *Cnnm4* (n=5) or an unrelated control (siCtrl) (n=5) were injected via tail vein injection and compared to control group (n=5). **A.** mRNA levels and protein expression levels of CNNM4. **B.** Liver necrosis was assessed by H&E staining. Scale bar correspond to 100 µm. **C.** Cell death was determined by TUNEL assay in liver tissue. Scale bar correspond to 100 µm. **D.**Transaminases ALT and AST levels were determined in mice serum. **E.** ROS *in vivo* measured by DHE staining in liver sections. Scale bar correspond to 100 µm. **F.** Inflammation assessed by F4/80 staining in liver. Scale bar correspond to 100 µm. **G.** Magnesium levels were determined in mice serum. **H-M** WT mice were treated with a single dose of APAP 360 mg/kg by intraperitoneal injection and 24h thereafter with 3mg/kg GalNAc *Cnnm4* siRNA (n=4) or a non targeting GalNAc conjugated control siRNA (n=4) were injected via subcutaneous injection. Mice were sacrificed 48h after APAP overdose. **H.** mRNA levels and protein expression of CNNM4 was determined. **I.** Liver necrosis was assessed by H&E staining at 48h after APAP overdose. **J.** Cell death was assessed by TUNEL assay. **K.** Transaminases ALT and AST levels were determined in mice serum at 48h after APAP overdose. **L.** Inflammation assessed by F4/80 staining in liver at 48h after APAP overdose. **M.** Magnesium levels were determined in mice serum at 48h of APAP overdose. Respective quantifications are represented as mean ± SEM. **P*<0.05, ***P*<0.01, ****P*<0.001 (Student's test).

Figure 6. CNNM4 silencing reduces ER stress induces by APAP overdose in *in vivo* models
Proteomics analysis by LC-MS/MS was assessed in the liver of WT mice treated with a single dose of 360mg/kg APAP and 24h after APAP overdose mice were injected with siRNA *Cnnm4* (n=7) or an unrelated control (siCtrl) (n=7). **A.** Volcano plot of specific proteins regulated by the absence of *Cnnm4* was shown. **B.** GO process analysis for the regulated genes in APAP+siCtrl vs APAP+si*Cnnm4* labelled (APAP+siCtrl) and in APAP+si*Cnnm4* vs APAP+siCtrl labelled (APAP + si*Cnnm4*). **C.** mRNA levels of *Atf-6, Chop, X-box binding protein 1 (Xbp1s/Xbp1u) and binding immunoglobulin protein (Grp78)* in WT mice treated with a single dose of APAP 360mg/kg and 24h after siRNA *Cnnm4* (n=5) or an unrelated control (n=5). **D.** Western blot analysis of phospho-EIF2α Ser 51 (p-EIF2α) and EIF2α ratio, β-ACTIN was used as a loading control. Quadrupled were used for experimental condition. **E.** mRNA levels of *Atf-6, Chop, X-box binding protein 1 (Xbp1s/Xbp1u) and binding immunoglobulin protein (Grp78)* in WT mice treated with a single dose of APAP 360mg/kg and 24h after with a *Cnnm4* GalNAc siRNA molecule (n=4) or an unrelated control (n=4). **F.** Western blot analysis of PERK, HSP90 was used as a loading control. Quadrupled were used for experimental condition. **G.** Celular location of CNNM4 in WT mice liver tissue with an APAP overdose 360mg/kg for 48h and compared with a healthy mice. Protein expression was measured in membrane, mitochondria an ER location. CD36, voltage-dependent anion channel (VDAC) and Calnexin (CANX) were used as a loading controls. Triplicates were used for experimental conditions. **H.** Basal respiration using seahorse assay in mitochondria extract from mice liver with and 360mg/kg of APAP overdose and 24h later, injected with 3mg/kg

GalNAc Cnnm4 or an unrelated control. **I-K** Hepatocytes isolated from WT mice treated with a single dose of APAP 360 mg/kg and 24h later, injected with 3mg/kg GalNAc *Cnnm4* or an unrelated control. **I.** The mitochondrial Reactive Oxygen Species was determined using MitoSOX staining **J.** ATP levels were measured. **K.** ER tracker red staining. Quadrupled were used for experimental conditions. Values are represented as mean ± SEM. **P* < 0.05, ***P* < 0.01, ***P*<0.001 (Student's test)

Figure 7. CNNM4 knockdown induced liver regeneration in preclinical APAP model.

A. mRNA levels of *Cyclin D1 and Cyclin D2 and* **B.** PCNA expression by immunohistochemistry. Scale bar corresponds to 50 µm in WT mice treated for 48 h with APAP (n=5) and silenced *Cnnm4* by siRNA the last 24 hours of the hepatotoxic (n=5). **C-D.** Changes in mRNA levels of Hepatocyte Growth Factor(*Hgf), Heparin Binding EGF Like Growth Factor (Hb-egf),* Epidermal Growth Factor *(Egf), Betacellulin (Btc), Betacellulin v2 (Btc2), Amphiregulin (Areg), Transforming Growth Factor Alpha (Tgfα) and Transforming Growth Factor Beta (Tgfβ)* in **(C)** WT mice treated with a single dose of APAP 360 mg/kg for 48h (n=5) and treated with a si*Cnnm4* for the last 24h (n=5) and **(D)** WT mice treated with a single dose of APAP 360 mg/kg for 36h (n=4) and treated with a *Cnnm4* GalNAc siRNA molecule the last 12h (n=4). **E.** mRNA expression levels of p21 was determined in WT mice with an APAP overdose for 36h (n=4) and treated with *Cnnm4* GalNAc siRNA molecule for 12h (n=4). **F.** Western blot analysis of Phospho cMET (Tyr 1230/ Tyr1234/ Tyr1235) in WT mice with an APAP overdose for 36h (n=4) and treated with *Cnnm4* GalNAc siRNA molecule for 12h (n=4). β-ACTIN was used as a loading control. Values are represented as mean ± SEM. **P* < 0.05, ***P* < 0.01, ***P*<0.001 (Student's test)

Figure 8. Overall mechanisms involved in CNNM4 overexpression caused by APAP overdose

In the liver, APAP overdose leads to increased expression of CNNM4 and an enrichment of its localization in the ER. Under these circumstances, reticulum stress and mitochondrial dysfunction are induced. The activity of CNNM4 is mainly influenced by its role as a magnesium effluxer. Therefore, increased CNNM4 expression reduces both mitochondrial and total cellular magnesium levels. When ER stress occurs, UPR markers, GRP78, ATF-6, PERK, pEIF2α, XBP1 and CHOP, are activated in order to solve the damage. Moreover IRE1α pathway triggers pJNK activation in order to induce apoptosis. pJNK is translocated to mitochondria resulting in mitochondrial ROS, mitochondrial dysfunction and consequently cell death. Another characteristic of ER stress is the Ca^{2+} released into the cytoplasm to induce apoptosis. Finally, inflammation markers such as TNF and IL6 are induced as a consequence of APAP overdose. Silencing of *Cnnm4* in the liver was able to reduce mitochondrial dysfunction, ER stress and induce a regenerative response in the hepatocyte to overcome APAP overdose-induced necrosis.

References

1. Cassidy, A. *et al.* Plasma adiponectin concentrations are associated with body composition and plant-based dietary factors in female twins. *J. Nutr.* **139**, 353–358 (2009).
2. Grubbs, R. D. Intracellular magnesium and magnesium buffering. *BioMetals* **15**, 251–259 (2002).
3. Shahi, A., Aslani, S., Ataollahi, M. & Mahmoudi, M. The role of magnesium in different inflammatory diseases. *Inflammopharmacology* **27**, 649–661 (2019).
4. Li, W. *et al.* Intakes of magnesium, calcium and risk of fatty liver disease and prediabetes. *Vic. Lit. Cult.* **21**, 2088–2095 (2018).
5. Liu, M., Yang, H. & Mao, Y. Magnesium and liver disease. *Ann. Transl. Med.* **7**, 578 (2019).
6. Zhang, G., Gruskos, J. J., Afzal, M. S. & Buccella, D. Visualizing changes in mitochondrial Mg2+ during apoptosis with organelle-targeted triazole-based ratiometric fluorescent sensors. *Chem. Sci.* **6**, 6841–6846 (2015).
7. Andrade, R. J. *et al.* Drug-induced liver injury. *Nat. Rev. Dis. Prim.* **5**, (2019).
8. Lee, W. M. Acetaminophen (APAP) hepatotoxicity—Isn't it time for APAP to go away? *J. Hepatol.* **67**, 1324–1331 (2017).
9. Bernal, W., Auzinger, G., Dhawan, A. & Wendon, J. Acute liver failure. *Lancet* **376**, 190–201 (2010).
10. Fisher, E. S. & Curry, S. C. *Evaluation and treatment of acetaminophen toxicity*. *Advances in Pharmacology* vol. 85 (Elsevier Inc., 2019).
11. Lee, W. M. *et al.* Intravenous N-Acetylcysteine Improves Transplant-Free Survival in Early Stage Non-Acetaminophen Acute Liver Failure. *Gastroenterology* **137**, 856-864.e1 (2009).
12. Barbier-Torres, L. *et al.* The mitochondrial negative regulator MCJ is a therapeutic target for acetaminophen-induced liver injury. *Nat. Commun.* **8**, 2068 (2017).
13. Jaeschke, H., Akakpo, J. Y., Umbaugh, D. S. & Ramachandran, A. Novel Therapeutic Approaches Against Acetaminophen-induced Liver Injury and Acute Liver Failure. *Toxicol. Sci.* **174**, 159–167 (2020).
14. Smilkstein, M. J., Knapp, G. L., Kulig, K. W. & Rumack, B. H. Efficacy of oral N-acetylcysteine in the treatment of acetaminophen overdose. Analysis of the national multicenter study (1976 to 1985). *N. Engl. J. Med.* **319**, 1557–1562 (1988).
15. Malhi, H. & Kaufman, R. J. Endoplasmic reticulum stress in liver disease. *J. Hepatol.* **54**, 795–809 (2011).

16. Rizzuto, R., De Stefani, D., Raffaello, A. & Mammucari, C. Mitochondria as sensors and regulators of calcium signalling. *Nat. Rev. Mol. Cell Biol.* **13**, 566–578 (2012).
17. Nagy, G. *et al.* Acetaminophen induces ER dependent signaling in mouse liver. *Arch. Biochem. Biophys.* **459**, 273–279 (2007).
18. Foufelle, F. & Fromenty, B. Role of endoplasmic reticulum stress in drug-induced toxicity. *Pharmacol. Res. Perspect.* **4**, 1–28 (2016).
19. Malhi, H. & Kaufman, R. J. Endoplasmic reticulum stress in liver disease. *J. Hepatol.* **54**, 795–809 (2011).
20. Sehgal, P. *et al.* Inhibition of the sarco/endoplasmic reticulum (ER) Ca2-ATPase by thapsigargin analogs induces cell death via ER Ca2 depletion and the unfolded protein response. *J. Biol. Chem.* **292**, 19656–19673 (2017).
21. Hur, K. Y. *et al.* IRE1 α activation protects mice against acetaminophen-induced hepatotoxicity. *J. Exp. Med.* **209**, 307–318 (2012).
22. Uzi, D. *et al.* CHOP is a critical regulator of acetaminophen-induced hepatotoxicity. *J. Hepatol.* **59**, 495–503 (2013).
23. Jaeschke, H. Glutathione disulfide formation and oxidant stress during acetaminophen-induced hepatotoxicity in mice in vivo: the protective effect of allopurinol. *J. Pharmacol. Exp. Ther.* **255**, 935–941 (1990).
24. Burcham, P. C. & Harman, A. W. Effect of acetaminophen hepatotoxicity on hepatic mitochondrial and microsomal calcium contents in mice. *Toxicol. Lett.* **44**, 91–99 (1988).
25. Kubota, T. *et al.* Mitochondria are intracellular magnesium stores: Investigation by simultaneous fluorescent imagings in PC12 cells. *Biochim. Biophys. Acta - Mol. Cell Res.* **1744**, 19–28 (2005).
26. Zsurka, G., Gregan, J. & Schweyen, R. J. The human mitochondrial Mrs2 protein functionally substitutes for its yeast homologue, a candidate magnesium transporter. *Genomics* **72**, 158–168 (2001).
27. Wang, C.-Y. *et al.* Molecular cloning and characterization of a novel gene family of four ancient conserved domain proteins (ACDP). *Gene* **306**, 37–44 (2003).
28. Fonfria, E. *et al.* Tissue distribution profiles of the human TRPM cation channel family. *J. Recept. Signal Transduct.* **26**, 159–178 (2006).
29. Quamme, G. A. Molecular identification of ancient and modern mammalian magnesium transporters. *Am. J. Physiol. Cell Physiol.* **298**, C407--29 (2010).
30. Simón, J. *et al. Magnesium accumulation upon cyclin M4 silencing activates microsomal triglyceride transfer protein improving NASH*. *Journal of Hepatology* (European Association for the Study of the Liver, 2021).

doi:10.1016/j.jhep.2021.01.043.

31. Hirata, Y., Funato, Y., Takano, Y. & Miki, H. Mg2+-dependent interactions of ATP with the cystathionine- β-synthase (CBS) domains of a magnesium transporter. *J. Biol. Chem.* **289**, 14731–14739 (2014).
32. Vadolas, J. *et al.* SLN124, a GalNac-siRNA targeting transmembrane serine protease 6, in combination with deferiprone therapy reduces ineffective erythropoiesis and hepatic iron-overload in a mouse model of β-thalassaemia. *Br. J. Haematol.* **194**, 200–210 (2021).
33. Romani, A. Regulation of magnesium homeostasis and transport in mammalian cells. *Arch. Biochem. Biophys.* **458**, 90–102 (2007).
34. Miki, H. Molecular functions of CNNM Mg 2＋ transporters and their biomedical importance. *Seikagaku* **90**, 444–451 (2018).
35. Iorga, A., Dara, L. & Kaplowitz, N. Drug-Induced Liver Injury: Cascade of Events Leading to Cell Death, Apoptosis or Necrosis. *Int. J. Mol. Sci.* **18**, (2017).
36. Weingärtner, A., Bethge, L., Weiss, L., Sternberger, M. & Lindholm, M. W. Less Is More: Novel Hepatocyte-Targeted siRNA Conjugates for Treatment of Liver-Related Disorders. *Mol. Ther. - Nucleic Acids* **21**, 242–250 (2020).
37. Funato, Y. *et al.* Membrane protein CNNM4 – dependent Mg 2 + efflux suppresses tumor progression Find the latest version : Membrane protein CNNM4 – dependent Mg 2 + efflux suppresses tumor progression. *J. Clin. Invest.* **124**, 5398–5410 (2014).
38. Wu, L. *et al.* Magnesium intake and mortality due to liver diseases: Results from the Third National Health and Nutrition Examination Survey Cohort. *Sci. Rep.* **7**, 1–6 (2017).
39. Gill, P. *et al.* MicroRNA regulation of CYP 1A2, CYP3A4 and CYP2E1 expression in acetaminophen toxicity. *Sci. Rep.* **7**, 1–11 (2017).
40. Jaeschke, H., Williams, C. D., Ramachandran, A. & Bajt, M. L. Acetaminophen hepatotoxicity and repair: The role of sterile inflammation and innate immunity. *Liver Int.* **32**, 8–20 (2012).
41. Yong, J. *et al.* Mitochondria supply ATP to the ER through a mechanism antagonized by cytosolic Ca2+. *Elife* **8**, 1–25 (2019).
42. Yamazaki, D. *et al.* Basolateral Mg2+ Extrusion via CNNM4 Mediates Transcellular Mg2+ Transport across Epithelia: A Mouse Model. *PLoS Genet.* **9**, (2013).
43. Afzal, M. S., Pitteloud, J. P. & Buccella, D. Enhanced ratiometric fluorescent indicators for magnesium based on azoles of the heavier chalcogens. *Chem. Commun.* **50**, 11358–11361 (2014).

44. Verma, G. & Datta, M. The critical role of JNK in the ER-mitochondrial crosstalk during apoptotic cell death. *J. Cell. Physiol.* **227**, 1791–1795 (2012).
45. Grynkiewicz, G., Poenie, M. & Tsien, R. Y. A new generation of Ca2+ indicators with greatly improved fluorescence properties. *J. Biol. Chem.* **260**, 3440–3450 (1985).
46. Thastrup, O., Cullen, P. J., Drobak, B. K., Hanley, M. R. & Dawson, A. P. Thapsigargin, a tumor promoter, discharges intracellular Ca2+ stores by specific inhibition of the endoplasmic reticulum Ca2+-ATPase. *Proc. Natl. Acad. Sci. U. S. A.* **87**, 2466–2470 (1990).
47. Lin, Y. P., Bakowski, D., Mirams, G. R. & Parekh, A. B. Selective recruitment of different Ca 2+-dependent transcription factors by STIM1-Orai1 channel clusters. *Nat. Commun.* **10**, (2019).
48. Wan, H. X., Hu, J. H., Xie, R., Yang, S. M. & Dong, H. Important roles of P2Y receptors in the inflammation and cancer of digestive system. *Oncotarget* **7**, 28736–28747 (2016).
49. Khodaee, N., Ghasemi, M., Saghiri, R. & Eliassi, A. Endoplasmic reticulum membrane potassium channel dysfunction in high fat diet induced stress in rat hepatocytes. *EXCLI J.* **13**, 1075–1087 (2014).
50. Nikam, R. R. & Gore, K. R. Journey of siRNA: Clinical Developments and Targeted Delivery. *Nucleic Acid Ther.* **28**, 209–224 (2018).
51. Bhushan, B. & Apte, U. Liver Regeneration after Acetaminophen Hepatotoxicity: Mechanisms and Therapeutic Opportunities. *Am. J. Pathol.* **189**, 719–729 (2019).
52. Marschall, H. U., Wagner, M., Zollner, G. & Trauner, M. Clinical hepatotoxicity. Regulation and treatment with inducers of transport and cofactors. *Mol. Pharm.* **4**, 895–910 (2007).
53. Centers, C. *et al.* Results of a Prospective Study of Acute Liver Failure at 17 Tertiary Care Centers in the United States. *Ann. Intern. Med.* **137**, 947–955 (2002).
54. Zolotarov, Y. *et al.* ARL15 modulates magnesium homeostasis through N-glycosylation of CNNMs. *Cell. Mol. Life Sci.* **78**, 5427–5445 (2021).
55. Yamazaki, D. *et al.* Cnnm4 deficiency suppresses Ca2+ signaling and promotes cell proliferation in the colon epithelia. *Oncogene* **38**, 3962–3969 (2019).
56. Morio, B., Panthu, B., Bassot, A. & Rieusset, J. Role of mitochondria in liver metabolic health and diseases. *Cell Calcium* **94**, (2021).
57. Bhushan, B. & Apte, U. Liver Regeneration after Acetaminophen Hepatotoxicity: Mechanisms and Therapeutic Opportunities. *Am. J. Pathol.* **189**, 719–729 (2019).
58. Goikoetxea-Usandizaga, N. *et al.* Mitochondrial bioenergetics boost macrophages

activation promoting liver regeneration in metabolically compromised animals. *Hepatology* (2021) doi:10.1002/HEP.32149.

59. Borude, P., Bhushan, B. & Apte, U. DNA damage response regulates initiation of liver regeneration following acetaminophen overdose. *Gene Expr.* **18**, 115–123 (2018).

60. Ramachandran, A. & Jaeschke, H. Oxidant Stress and Acetaminophen Hepatotoxicity: Mechanism-Based Drug Development. *Antioxid. Redox Signal.* **35**, 718–733 (2021).

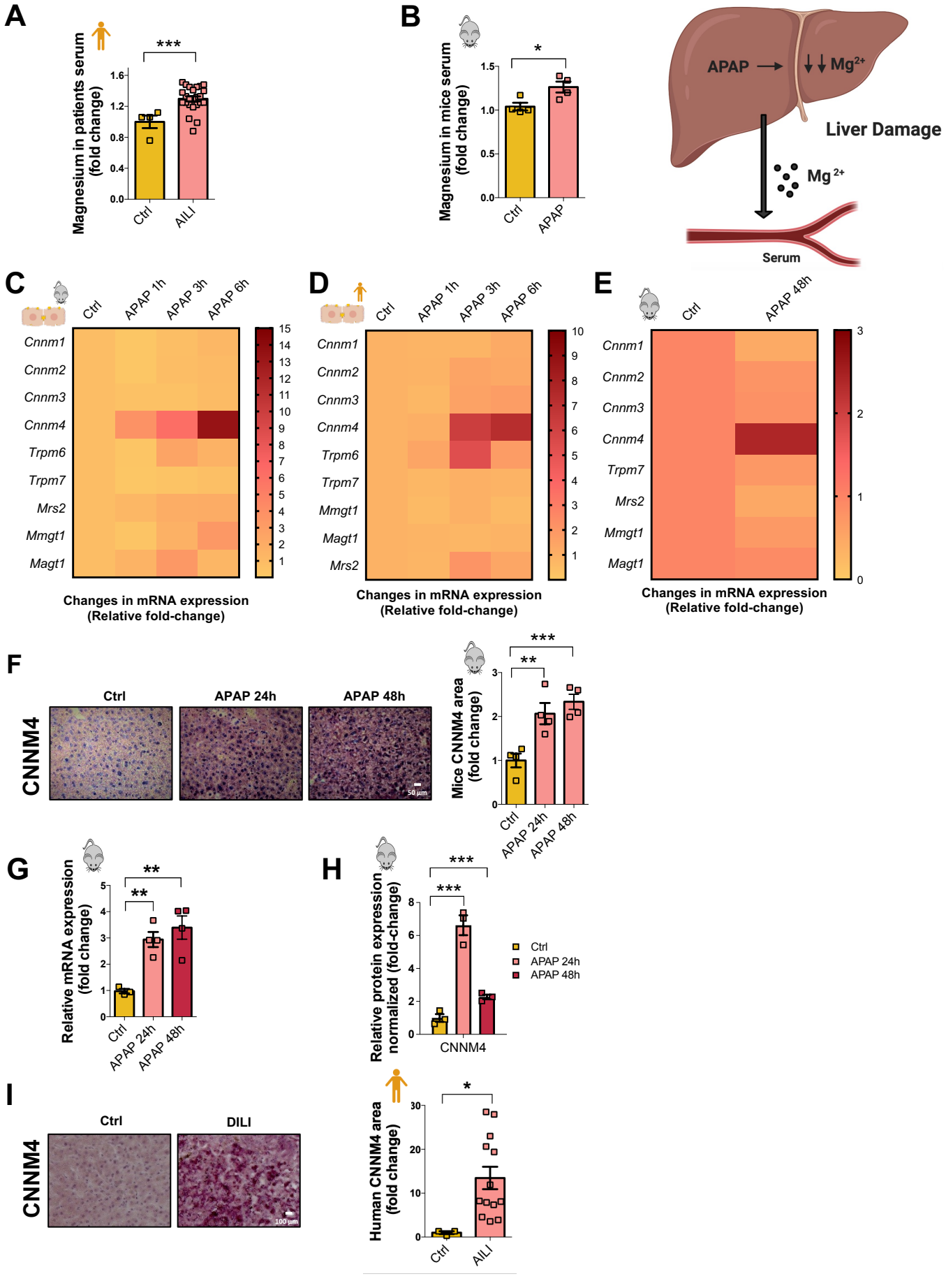
A
Magnesium in patients serum (fold change)
***
Ctrl
AILI
B
Magnesium in mice serum (fold change)
*
Ctrl
APAP
APAP
Mg2+
Liver Damage
Mg 2+
Serum
C
Ctrl
APAP 1h
APAP 3h
APAP 6h
Cnnm1
Cnnm2
Cnnm3
Cnnm4
Trpm6
Trpm7
Mrs2
Mmgt1
Magt1
Changes in mRNA expression (Relative fold-change)
D
Ctrl
APAP 1h
APAP 3h
APAP 6h
Cnnm1
Cnnm2
Cnnm3
Cnnm4
Trpm6
Trpm7
Mmgt1
Magt1
Mrs2
Changes in mRNA expression (Relative fold-change)
E
Ctrl
APAP 48h
Cnnm1
Cnnm2
Cnnm3
Cnnm4
Trpm7
Mrs2
Mmgt1
Magt1
Changes in mRNA expression (Relative fold-change)
F
CNNM4
Ctrl
APAP 24h
APAP 48h
50 µm
Mice CNNM4 area (fold change)
***
**
Ctrl
APAP 24h
APAP 48h
G
Relative mRNA expression (fold change)
**
**
Ctrl
APAP 24h
APAP 48h
H
Relative protein expression normalized (fold-change)
***
***
CNNM4
Ctrl
APAP 24h
APAP 48h
I
CNNM4
Ctrl
DILI
100 µm
Human CNNM4 area (fold change)
*
Ctrl
AILI

FIGURE 2

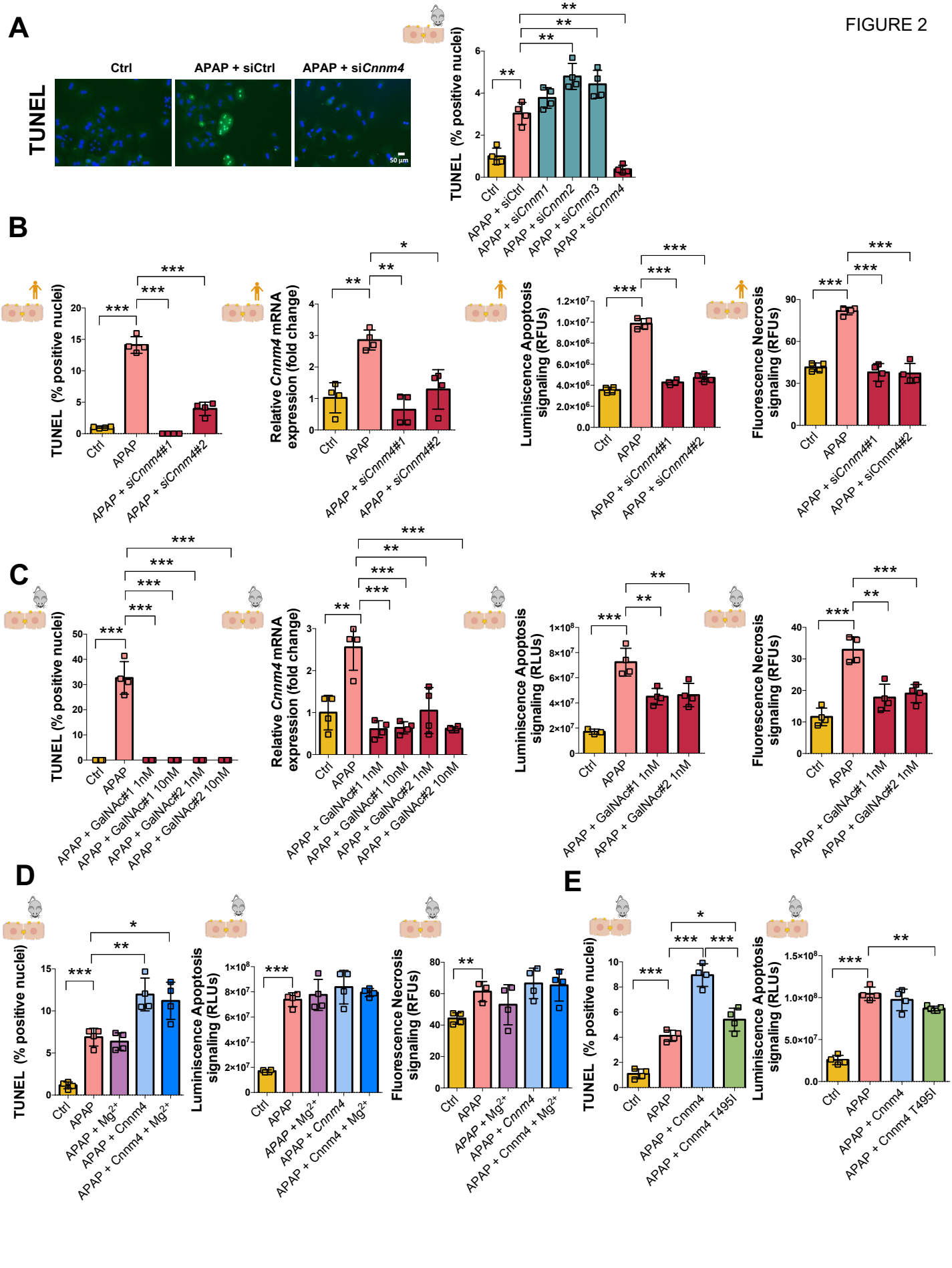
A
TUNEL
Ctrl
APAP + siCtrl
APAP + siCnnm4
50 μm
TUNEL (% positive nuclei)
Ctrl
APAP + siCtrl
APAP + siCnnm1
APAP + siCnnm2
APAP + siCnnm3
APAP + siCnnm4
B
TUNEL (% positive nuclei)
Relative Cnnm4 mRNA expression (fold change)
Luminiscence Apoptosis signaling (RFUs)
Fluorescence Necrosis signaling (RFUs)
Ctrl
APAP
APAP + siCnnm4#1
APAP + siCnnm4#2
C
TUNEL (% positive nuclei)
Relative Cnnm4 mRNA expression (fold change)
Luminiscence Apoptosis signaling (RLUs)
Fluorescence Necrosis signaling (RFUs)
Ctrl
APAP
APAP + GalNAc#1 1nM
APAP + GalNAc#1 10nM
APAP + GalNAc#2 1nM
APAP + GalNAc#2 10nM
D
TUNEL (% positive nuclei)
Luminiscence Apoptosis signaling (RLUs)
Fluorescence Necrosis signaling (RFUs)
Ctrl
APAP
APAP + Mg2+
APAP + Cnnm4
APAP + Cnnm4 + Mg2+
E
TUNEL (% positive nuclei)
Luminiscence Apoptosis signaling (RLUs)
Ctrl
APAP
APAP + Cnnm4
APAP + Cnnm4 T495I

FIGURE 3

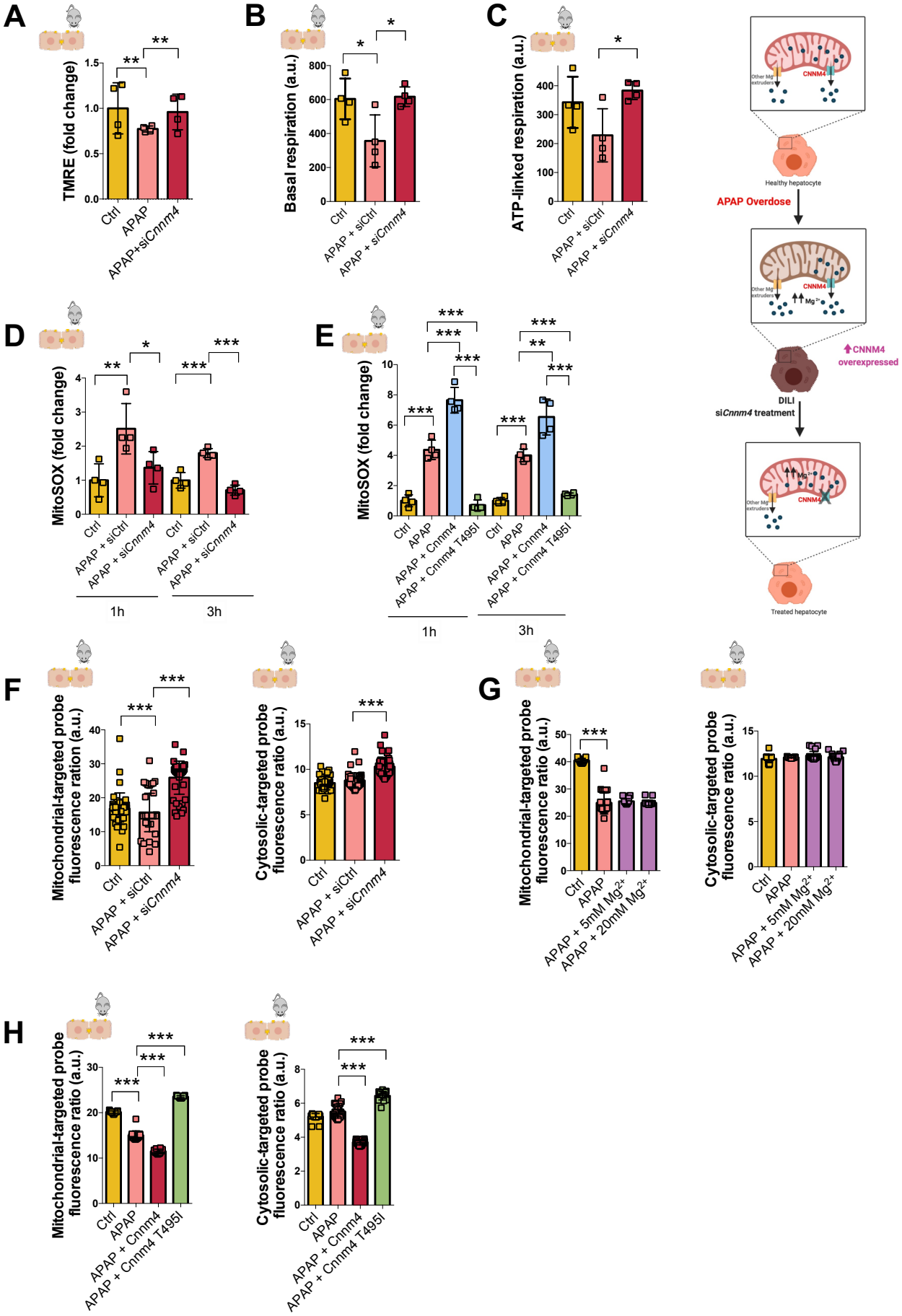
A
TMRE (fold change)
Ctrl
APAP
APAP+siCnnm4
B
Basal respiration (a.u.)
Ctrl
APAP + siCtrl
APAP + siCnnm4
C
ATP-linked respiration (a.u.)
Ctrl
APAP + siCtrl
APAP + siCnnm4
Other Mg2+ extruders
CNNM4
Healthy hepatocyte
APAP Overdose
Mg2+
CNNM4 overexpressed
DILI
siCnnm4 treatment
Treated hepatocyte
D
MitoSOX (fold change)
Ctrl
APAP + siCtrl
APAP + siCnnm4
1h
3h
E
MitoSOX (fold change)
Ctrl
APAP
APAP + Cnnm4
APAP + Cnnm4 T495I
1h
3h
F
Mitochondrial-targeted probe fluorescence ration (a.u.)
Ctrl
APAP + siCtrl
APAP + siCnnm4
Cytosolic-targeted probe fluorescence ratio (a.u.)
Ctrl
APAP + siCtrl
APAP + siCnnm4
G
Mitochondrial-targeted probe fluorescence ratio (a.u.)
Ctrl
APAP
APAP + 5mM Mg2+
APAP + 20mM Mg2+
Cytosolic-targeted probe fluorescence ratio (a.u.)
Ctrl
APAP
APAP + 5mM Mg2+
APAP + 20mM Mg2+
H
Mitochondrial-targeted probe fluorescence ratio (a.u.)
Ctrl
APAP
APAP + Cnnm4
APAP + Cnnm4 T495I
Cytosolic-targeted probe fluorescence ratio (a.u.)
Ctrl
APAP
APAP + Cnnm4
APAP + Cnnm4 T495I

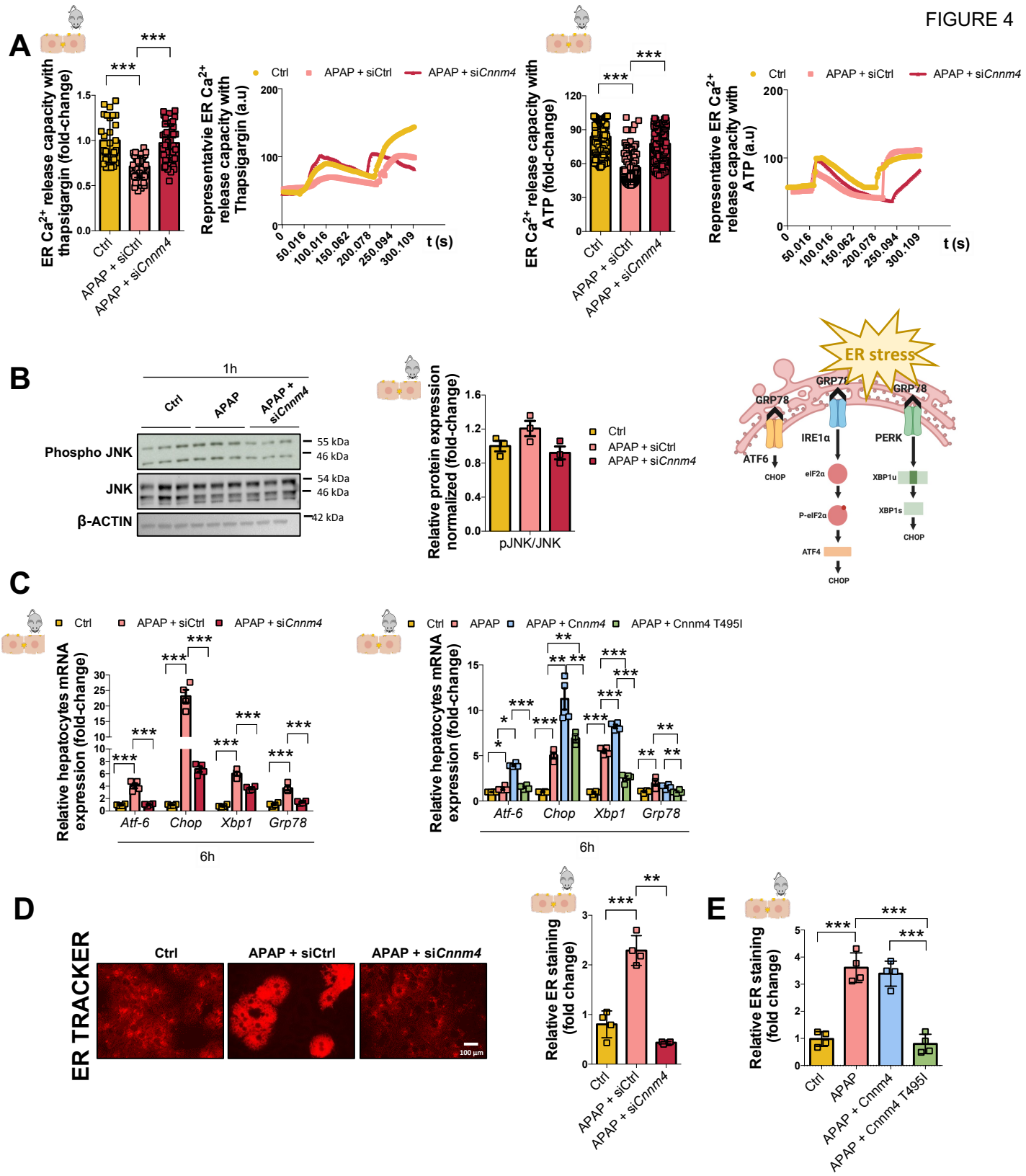
A
ER Ca2+ release capacity with thapsigargin (fold-change)
Ctrl
APAP + siCtrl
APAP + siCnnm4
Representative ER Ca2+ release capacity with Thapsigargin (a.u)
t (s)
ER Ca2+ release capacity with ATP (fold-change)
Representative ER Ca2+ release capacity with ATP (a.u)
B
1h
Phospho JNK
JNK
β-ACTIN
55 kDa
46 kDa
54 kDa
42 kDa
Relative protein expression normalized (fold-change)
pJNK/JNK
ER stress
GRP78
IRE1α
PERK
ATF6
CHOP
eIF2α
P-eIF2α
ATF4
XBP1u
XBP1s
C
APAP + Cnnm4
APAP + Cnnm4 T495I
Relative hepatocytes mRNA expression (fold-change)
Atf-6
Chop
Xbp1
Grp78
6h
D
ER TRACKER
100 µm
Relative ER staining (fold change)
E

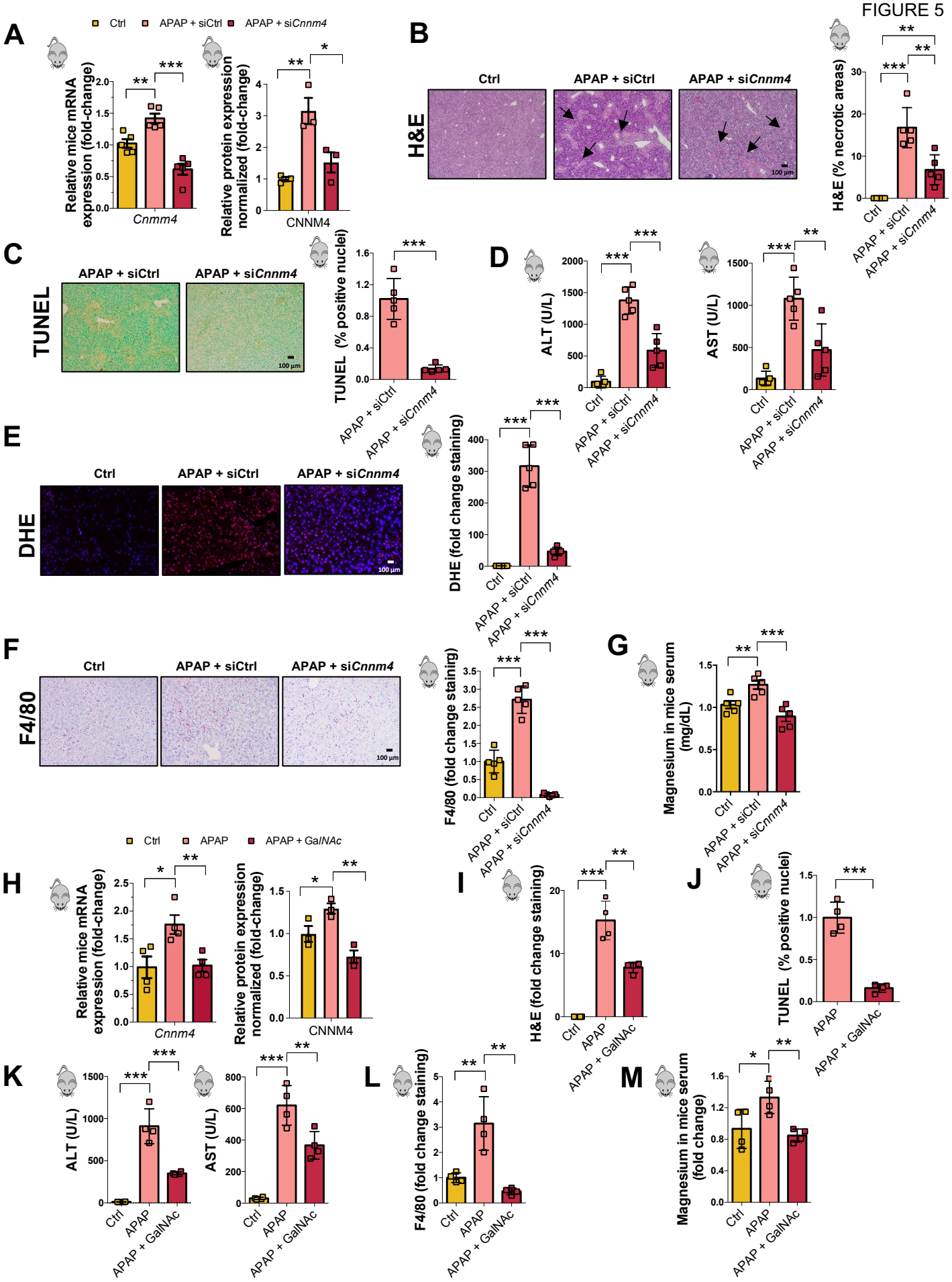
A
Ctrl
APAP + siCtrl
APAP + siCnnm4
Relative mice mRNA expression (fold-change)
Cnmm4
Relative protein expression normalized (fold-change)
CNNM4
B
H&E
Ctrl
APAP + siCtrl
APAP + siCnnm4
100 µm
H&E (% necrotic areas)
C
TUNEL
APAP + siCtrl
APAP + siCnnm4
100 µm
TUNEL (% positive nuclei)
D
ALT (U/L)
AST (U/L)
E
DHE
Ctrl
APAP + siCtrl
APAP + siCnnm4
100 µm
DHE (fold change staining)
F
F4/80
Ctrl
APAP + siCtrl
APAP + siCnnm4
100 µm
F4/80 (fold change stainirg)
G
Magnesium in mice serum (mg/dL)
Ctrl
APAP
APAP + GalNAc
H
Relative mice mRNA expression (fold-change)
Cnnm4
Relative protein expression normalized (fold-change)
CNNM4
I
H&E (fold change staining)
J
TUNEL (% positive nuclei)
K
ALT (U/L)
AST (U/L)
L
F4/80 (fold change staining)
M
Magnesium in mice serum (fold change)

FIGURE 6

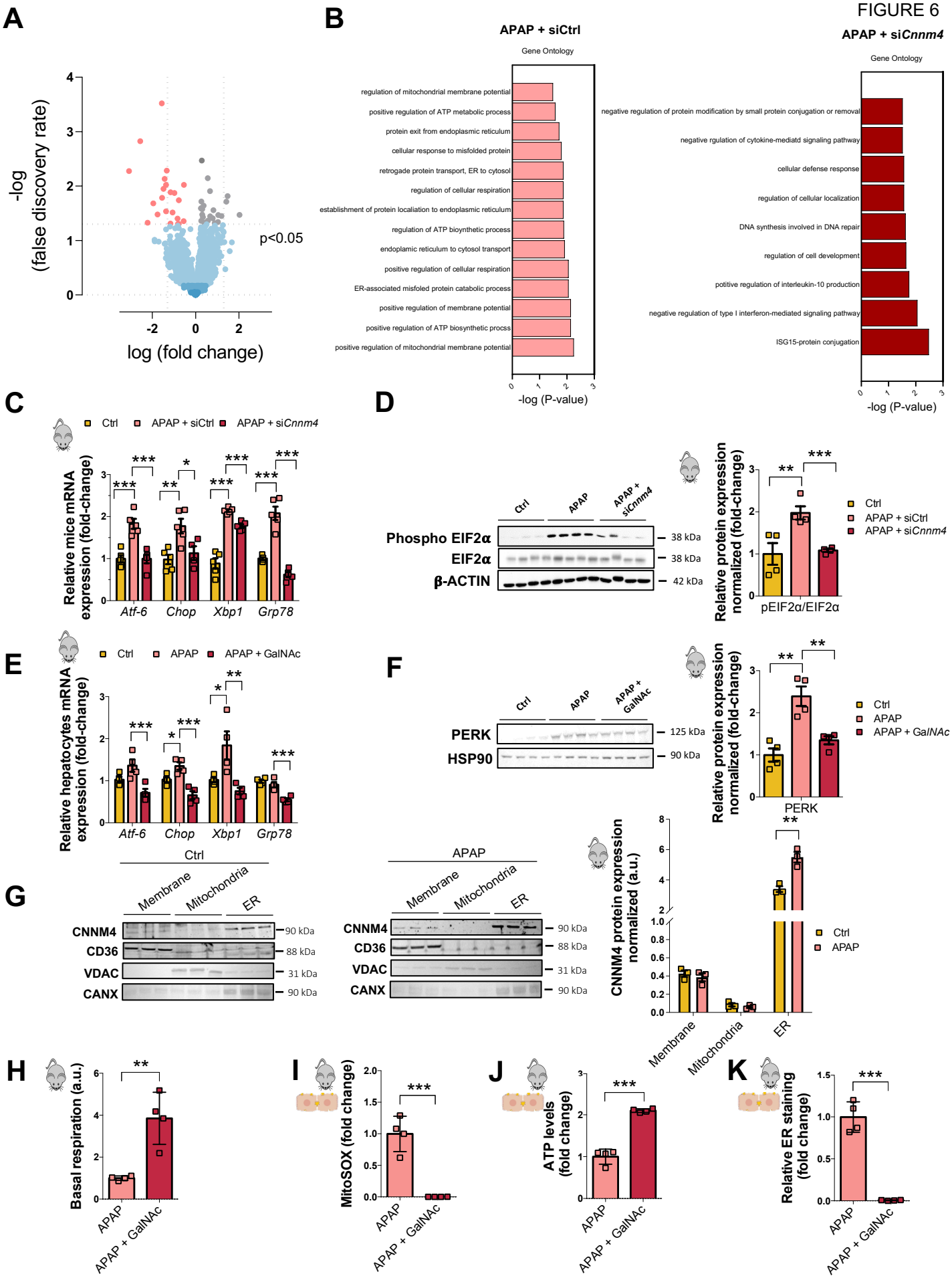
A
-log (false discovery rate)
log (fold change)
p<0.05
B
APAP + siCtrl
Gene Ontology
regulation of mitochondrial membrane potential
positive regulation of ATP metabolic process
protein exit from endoplasmic reticulum
cellular response to misfolded protein
retrogade protein transport, ER to cytosol
regulation of cellular respiration
establishment of protein localiation to endoplasmic reticulum
regulation of ATP bioynthetic process
endoplamic reticulum to cytosol transport
positive regulation of cellular respiration
ER-associated misfoled protein catabolic process
positive regulation of membrane potential
positive regulation of ATP biosynthetic procss
positive regulation of mitochondrial membrane potential
-log (P-value)
APAP + siCnnm4
Gene Ontology
negative regulation of protein modification by small protein conjugation or removal
negative rgulation of cytokine-mediatd signaling pathway
cellular defense response
regulation of cellular localization
DNA synthesis involved in DNA repair
regulation of cell development
potitive regulation of interleukin-10 production
negative regulation of type I interferon-mediated signaling pathway
ISG15-protein conjugation
-log (P-value)
C
Ctrl
APAP + siCtrl
APAP + siCnnm4
Relative mice mRNA expression (fold-change)
Atf-6
Chop
Xbp1
Grp78
D
Ctrl
APAP
APAP + siCnnm4
Phospho EIF2α
EIF2α
β-ACTIN
38 kDa
38 kDa
42 kDa
Relative protein expression normalized (fold-change)
pEIF2α/EIF2α
Ctrl
APAP + siCtrl
APAP + siCnnm4
E
Ctrl
APAP
APAP + GalNAc
Relative hepatocytes mRNA expression (fold-change)
Atf-6
Chop
Xbp1
Grp78
F
Ctrl
APAP
APAP + GalNAc
PERK
HSP90
125 kDa
90 kDa
Relative protein expression normalized (fold-change)
PERK
Ctrl
APAP
APAP + GalNAc
G
Ctrl
APAP
Membrane
Mitochondria
ER
CNNM4
CD36
VDAC
CANX
90 kDa
88 kDa
31 kDa
90 kDa
CNNM4 protein expression normalized (a.u.)
Membrane
Mitochondria
ER
Ctrl
APAP
H
Basal respiration (a.u.)
APAP
APAP + GalNAc
I
MitoSOX (fold change)
APAP
APAP + GalNAc
J
ATP levels (fold change)
APAP
APAP + GalNAc
K
Relative ER staining (fold change)
APAP
APAP + GalNAc

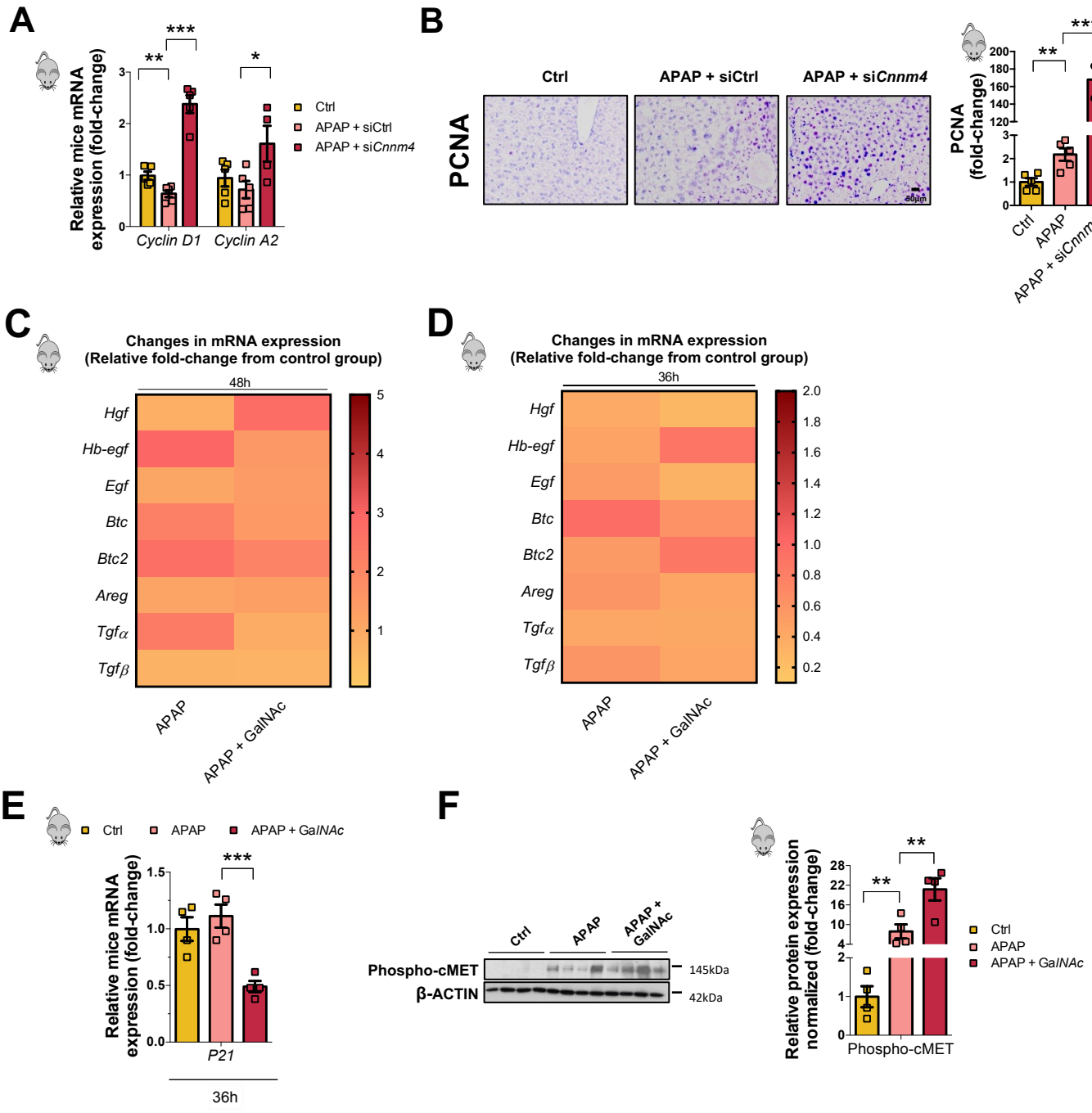
A
Relative mice mRNA expression (fold-change)
Cyclin D1
Cyclin A2
Ctrl
APAP + siCtrl
APAP + siCnnm4
B
PCNA
Ctrl
APAP + siCtrl
APAP + siCnnm4
PCNA (fold-change)
C
Changes in mRNA expression
(Relative fold-change from control group)
48h
Hgf
Hb-egf
Egf
Btc
Btc2
Areg
Tgfα
Tgfβ
APAP
APAP + GalNAc
D
Changes in mRNA expression
(Relative fold-change from control group)
36h
E
Ctrl
APAP
APAP + GalNAc
Relative mice mRNA expression (fold-change)
P21
36h
F
Phospho-cMET
β-ACTIN
145kDa
42kDa
Relative protein expression normalized (fold-change)

FIGURE 8

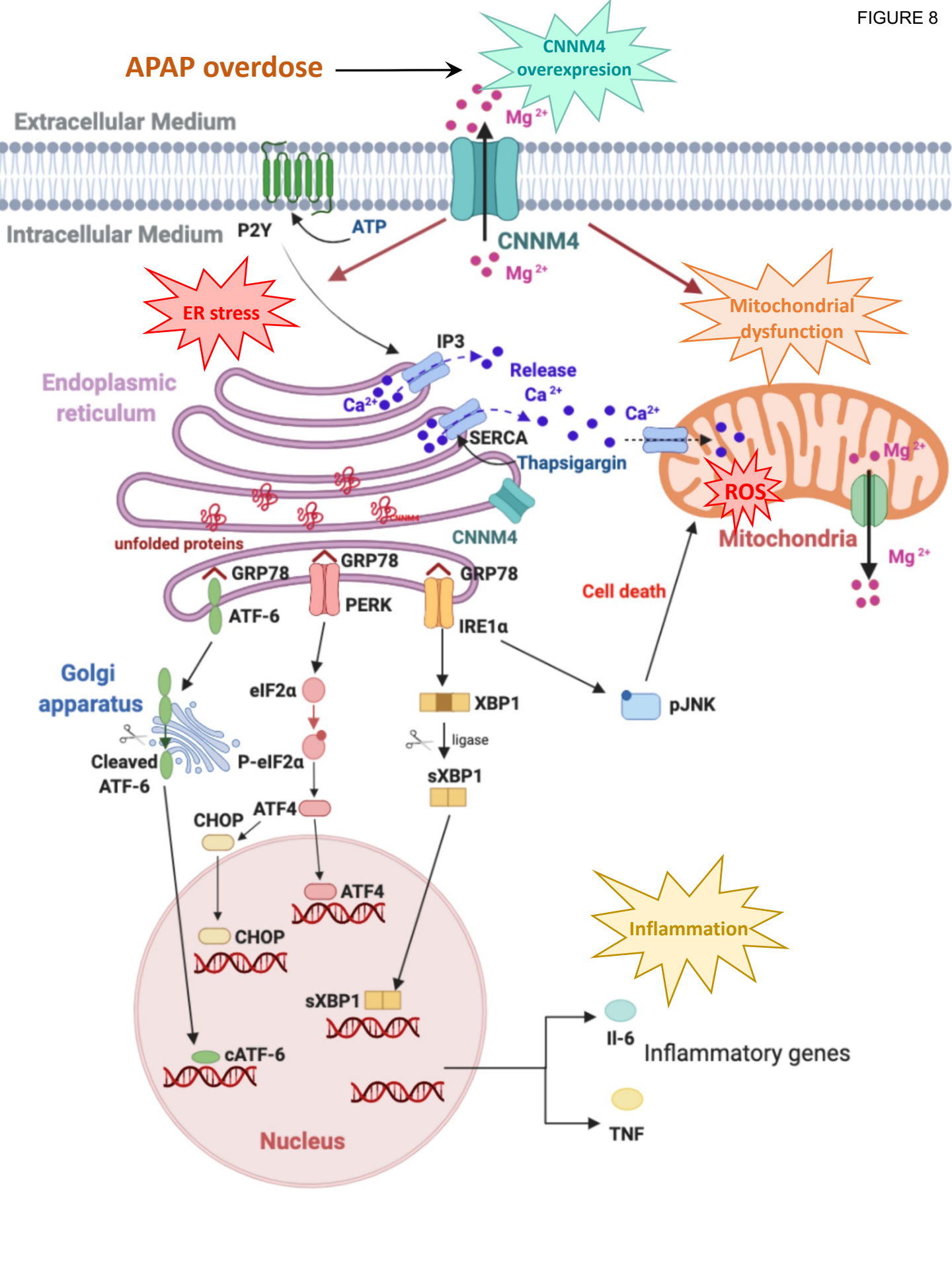
APAP overdose
CNNM4 overexpresion
Mg 2+
Extracellular Medium
Intracellular Medium
P2Y
ATP
CNNM4
Mg 2+
ER stress
Mitochondrial dysfunction
IP3
Release
Ca2+
Endoplasmic reticulum
Ca2+
Ca2+
SERCA
Thapsigargin
Mg 2+
ROS
Mitochondria
Mg 2+
unfolded proteins
CNNM4
GRP78
GRP78
GRP78
ATF-6
PERK
IRE1α
Cell death
Golgi apparatus
eIF2α
XBP1
pJNK
ligase
Cleaved ATF-6
P-eIF2α
sXBP1
CHOP
ATF4
ATF4
CHOP
sXBP1
Inflammation
cATF-6
Il-6
Inflammatory genes
TNF
Nucleus